IMAGE APPROXIMATION USING EASY PATH WAVELET TRANSFORM

by

Maj Ajlaan Bin Mamoon

A thesis submitted to the faculty of Electrical Engineering Department Military College of Signals, National University of Sciences and Technology, Rawalpindi in partial fulfilment of the requirements for the degree of MS in Electrical Engineering

January 2017

ABSTRACT

Everyday an enormous amount of information is stored, processed, and transmitted. Because much of this information is graphical or pictorial in nature, the storage and communications requirements are immense. Though in recent time's bandwidth capacities got much higher and cost of mass storage space got lower but still a lot of problems are faced during transmitting and storing images. Image compression plays vital role in terms of saving storage space and reduction of transmission time. Wavelet transform is considered as landmark in the field of image compression due to the feature that it represents a signal in terms of functions those are localized in both frequency and time domain, as not in case of other Transformation techniques. Various techniques have been explored by different authors to employ wavelet transform for image compression e.g. EZW, SPIHT etc. The idea of any scheme is to remove the correlation present in the data. Tensor product orthogonal wavelet bases are unable to adapt towards directional geometric features.

The purpose of this work is to develop an algorithm that exploits spatial correlation between pixel values and then compresses the image using wavelet transform. Images are connected regions of similar texture and intensity levels that combine to form objects. Typically, magnitude of pixels relate very closely to each other, thereby having less difference between them. Main idea is what already suggested in chain codes but contrary to it encoding is with respect to direction. Applying such a technique reduces entropy of geometrical features.

ACKNOWLEDGMENTS

I am thankful to my supervisor Colonel Dr Imran Touqir, Associate professor, Electrical Engineering Department Military College of Signals for his extraordinary and wholehearted support. He encouraged and kept me motivated despite my gradual pace due to health conditions. I am also thankful to my guidance committee members Lieutenant Col Dr Adnan Rashdi and Colonel Dr Imran Rashid HoD Electrical Engineering Department (B-Division) for their able guidance throughout the thesis process.

Finally, this work would have never materialized, had there been no consistent prayers, never ending love, support and encouragement of my mother and my wife.

LIST OF ACRONYMS

Acronym	Meaning
WT	Wavelet Transform
1D	One Dimensional
2D	Two Dimensional
SNR	Signal to Noise Ratio
PSNR	Peak Signal to Noise Ratio
DWT	Discrete Wavelet Transform
IDWT	Inverse Discrete Wavelet Transform
QMF	Quadrature Mirror Filter
DT	Discrete Transform
EPWT	Easy Path Wavelet Transform

Table of Contents

LIST OF FIGURES

Figure Number **Page**

CHAPTER 1
INTRODUCTION

1.1. Background

Digital images play an important role both in daily life applications such as satellite television, magnetic resonance imaging, computer tomography as well as in areas of research and technology such as geographical information systems and astronomy. Image compression has broad applications in rising areas of multimedia database, medical imaging diagnosis and worldwide web (www). As we know that web contents are principally comprises on images so in order to deal with it image compression is a counterpart. So image compression is a challenging field for all researchers Image compression plays vital role in terms of saving storage space and reduction of transmission time. Wavelet transform is considered as landmark in the field of image compression due to the feature that it represents a signal in terms of functions those are localized in both frequency and time domain, as not in case of other transformation techniques.

Wavelet theory has great application in digital image processing. Wavelets are developed by Morlet and Grossman. The relationship between wavelets and filter banks is developed by French researchers Meyer, Mallat and Cohen [3], this theory is now used in most of technical work. The main application of wavelet transform is image or signal compression.

The Daubechies [5] work is useful for those who have limited knowledge of wavelets and mathematics. Wavelet transform is very useful and interesting tool for investigating images. Wavelet transform overcome the limitation of Fourier transform. Fourier transform shows the signal only in time domain or in frequency domain. It only shows the global information of the signal. A mother wavelet whose mean is zero have all its energy in time domain and is well observed by time varying signals. Scaling and wavelets function are basis function in wavelet transforms. Mallat [6] multi resolution representation theory allowed researchers to create their own family of wavelets on the specific criteria. The usefulness of DWT over other transformation is because it shows time frequency localization.

EPWT works on the principle of correlation between pixel values of geometric figures in natural images and exploits them.

Image compression is a technique in which we shrink the image size by, taking into account that there would be no consequence on the quality of the image. Image compression not only helps us to store the images in less disk space and save a lot

of memory, rather than it provides us the facility in transmission and reception of the image in smaller time. To achieve this compression there are lot of techniques to implement. Internet utilize the famous technique i.e. JPEG.

Compression of a digital image and compression of raw binary data are two separate things. If we compress digital image by using traditional image compression methods (normally used for raw binary data), this does not present good compression ratios and other compression measurement parameters. So there is need for those image compression techniques in which we could exploit the spatial features. If in some cases where quality is not big issue we can compress image by ignoring some details of the image, this technique known as Lossy compression.

At this stage we can observe compression in two different types, i.e. Lossy and lossless image compression techniques. In some situations where image quality and all details are key factors and can't be compromised, we use lossless image compression techniques. But the focus of researchers is on the Lossy image compression algorithms rather than lossless techniques, because most of the images are related to less sensitive human vision.

A tremendous progress is observed in the field of image compression in last three decades. Researchers are facilitated by the advent of Wavelet Transform. In which we get the details of the images, and get success in exploiting the spatial features and characteristics. There are lots of image compressions algorithms which are based on Wavelet transform. In [4] Shapiro familiarize with the embedded-zero-tree wavelet (EZW). It is a progressive image compression technique, in which embedded bits stream comes out. This extensive work is extended in [22] by A. Said and W.A.Pearlman and brought a new idea of image compression, by employing the concept of spatial orientation trees, named Set Partitioning in Hierarchical Trees (SPIHT).

1.2. Motivation of Research

This research is intended to develop a novel algorithm employing wavelet transform which can remove redundancy from images. Several factors are motivating this research; image compression is very obligatory in storing an image and. Although capacities of transmission lines got much higher and cost of mass storage space got lower in recent years, there are still a lot of problems transmitting and storing images. For example to save an image of size 1024 X 1024 on the disk space requires nearly equal to 3MB. In addition time compulsory to transmit this image through ISDN network is 7 minutes. On the other hand by employing the

proper compression techniques we can store the same image on 300KB disk space and reducing the transmission time up to 6sec. Delay enhances as we increase the size of the file to be transmitted. So compression becomes compulsory, when we are dealing with huge amount of data, without influencing the quality of digital image prior to storing/transmitting it. At receiving stage this compressed data is decompressed.

1.3. Problem Statement

Presently, there are many image compression techniques both in spatial and transform domain. Each technique performs outstandingly in removal of image compression of a particular type but fails to perform compress geometric features. The purpose is to develop a novel image compression technique employing wavelet transform which can perform satisfactorily on compress images.

1.4. Objectives of Research

This research is intended for literature review of the research work already done on image compression specialy in wavelet transform domain & then to develop an new method for image compression in order to compare the performance parameters like Disk saving capability in terms of no. of bits saving, Compression Ratio (CR), PSNR performance with exisiting compression algorithms.

1.5. Organization of Thesis Document

Chapter 1 introduces image compression importance and some research background as well as motivations of research and problem statement is also defined. Goal, objectives and scopes of research are stated clearly.

In Chapter 2 brief literature review of wavelets and subband coding techniques.

Chapter 3 and chapter 4 define in depth detail of proposed algorithum with test matrix.

Chapter 4 delineates experimental results based on the proposed algorithm and their analysis in detail.

Chapter 5 includes experimental results by taking different sample images

Chapter 6 proposes future work and conclusion.

Literature review

CHAPTER 2
WAVELET ANALYSIS

2.1 Evolution of Wavelets

The road towards the wavelets started with Josef Fourier with his research on frequency analysis. The term wavelets was first mentioned by Haar in 1909 and introduced compactly supported Haar wavelet. However, it was not perceived at that time that the wavelets will be established so strongly in mathematics, modern physics and engineering disciplines. The researchers in 1930 molded the research direction [2] from frequency analysis into scale analysis. Paul Levy found that in order to investigate small and complex details, Haar has more flexible and advantageous basis over Fourier. Littlewood, Paley, and Stein proved the energy conservation of the signal is domain independent led Davis Mar in 1980 to introduce an effective way to use the wavelets in Digital Image Processing applications. Since then various types of wavelet transforms have been developed and many other applications have been found. The continuous wavelet transform (CWT) finds out most of its applications in data analysis where it yields an affine invariant time frequency representation. DWT is however, the most popular. It has excellent signal compaction properties for many classes of real world signals while being computationally very efficient. Therefore, it has been applied to almost all technical fields including edge detection, image segmentation, compression, denoising, Pattern recognition and numerical integration. The theory of wavelets can be evolved from different approaches. Fourier transform constitutes fixed bases with infinite support. It is localized in frequency but does not provide space or time information of the signal. The widowing approach of Fourier transform known as short time Fourier transforms (STFT) is a trade off between localization of frequency and time. It does not give flexibility to application to change the resolution as per requirements. Therefore, it is not well adapted to isolate local singularities. It leads to more general and flexible approach in which analysis at different resolution and details can be made. A function can be analyzed by taking its projection on a single prototype function along its translations and scaling such that the prototype function obeys certain mathematical criteria. This phenomenon results in CWT. If the said basis function is discretized and then the signal is analyzed, it is termed as discrete time wavelet transforms. If the translations are integer multiples of two then it results in well known dyadic wavelet transform. Another approach is based on multi resolution approach which states that any lower dimensional signal can be represented by its

higher dimension or a higher dimensional signal can be represented by lower dimension signal along its orthogonal complement. The appeal of such an approach known as MRA facilitates retention of structural contents that might go undetected at one resolution may be easy to spot at another. However wavelets could not be effectively used till Mallat discovered that dyadic wavelets can be implemented by filter banks. Implementation of wavelets has its roots in subband coding. In the subsequent sections each aspect of wavelets will be briefly explained.

2.2 Short Time Fourier Transform

Fourier representation of signals is known to be effective in analysis of stationary periodic signals and not advocated for dynamic signals. STFT restricts the signal to an interval by multiplying it by a fixed window function, before carrying out a Fourier analysis of the product. Repeating the process with translated versions of window function allows localized frequency information throughout the signal to be obtained. Since the window width is same for all the frequencies, the amount of localization remains constant for different frequencies. STFT can be mathematically defined as

$$F(w,t) = \int_{t=-\infty}^{t=\infty} f(t) g^*_{w,t}(t) dt \tag{2.1}$$

where

$$g_{w,t} = \omega(t-\tau) e^{j\omega t} \tag{2.2}$$

The function *ω(t)* is a windowing function, the simplest of which is a rectangular window that has a unit value over a finite interval and is zero elsewhere.

2.3 Continuous Time Wavelet Transform

In contrast to sinusoidal function, a wavelet is a small wave whose energy is concentrated in time. Wavelets [7], [18], [19], [20], [21] are functions generated from one single function called mother wavelet by dilatations and translations in time domain. A wavelet denoted by *Ψ(t)* should have zero average value and unit energy.

$$\int_{-\infty}^{\infty} \varphi(t) dt = 0 \tag{2.3}$$

$$\int_{-\infty}^{\infty} |\varphi(t)|^2 dt = 1 \tag{2.4}$$

This guarantees its oscillating behaviour. The shifted and scaled wavelets *Ψa,b(t)* can be represented as:-

$$\varphi_{a,b} = |a|^{-1/2} \varphi\left(\frac{t-b}{a}\right) \tag{2.5}$$

Where a and b are two arbitrary real numbers and represent dilations and translations respectively. The pre factor $|a|^{-1/2}$ is normalization constant and responsible to ensure that all scaled functions$|a|^{-\frac{1}{2}}\varphi^*(\frac{t}{a})$ with *aεR* have the same energy. Thus the wavelet transform of a signal is computed as a collection of inner products of the signal and translated and scaled versions of a mother wavelet ψ(t) which can be written as

$$\omega_f(a,b) = \langle f, \varphi_{a,b} \rangle \tag{2.6}$$

Based on this definition, the wavelet transform of a function *f(t)* can be expanded as

$$\omega_f(a,b) = \int_{-\infty}^{\infty} f(t) \varphi_{a,b}^*(t) dt \tag{2.7}$$

Since the analysis function ψ(t) is scaled and not modulated like the kernel of STFT, a wavelet analysis is often called time scale analysis rather than time frequency analysis. For the existence of its inverse, the admissibility condition must be met i.e.

$$\int_{-\infty}^{\infty} \frac{|\varphi(\omega)|^2}{|\omega|} d\omega \ < \infty \tag{2.8}$$

where Ψ(ω) is the Fourier transform of mother wavelet *Ψ(t).* The inverse transform to reconstruct *f(t)* from $\omega_f(a,b)$ is represented as

$$f(t) = \frac{1}{c} \int_{-\infty}^{\infty} \int_{-\infty}^{\infty} \omega_f(a,b) \varphi_{a,b}(t) da db \tag{2.9}$$

where

$$c = \int_{-\infty}^{\infty} \frac{|\varphi(\omega)|^2}{|\omega|} d\omega \tag{2.10}$$

ψ(t) is equipped with vanishing moments, so there must be some function say φ(t) with non vanishing mean such that the former is the derivative of later

$$\varphi(t) = \frac{d\varphi(t)}{dt} \tag{2.11}$$

Φ(t) is called as father wavelet which can be similarly scaled and translated on continuous scale such that the energy remains unity.

$$\varphi_{a,b} = |a|^{-1/2}\varphi\left(\frac{t-b}{a}\right) \tag{2.12}$$

However the relation between father and mother wavelets will be refined in section 2.5 with the help of nested spaces.

CWT is highly redundant and the scales are taken on real axis which is unsuitable for digital processing. If small scales are taken with integer translation at each scale then it is termed as discrete time wavelet transform.

2.4 Discrete Time Wavelet Transform

Since image is processed by a digital computing machine, it is prudent to discretize *a* and *b* and then represent the discrete wavelets accordingly [8]. The generally appreciated approach of discretizing *a* and *b* is

$$a = a_0^m, m \in \mathbb{Z} \tag{2.13}$$

$$b = nb_0a_0^m, m \in \mathbb{Z} \tag{2.14}$$

Hence the wavelets can be represented as

$$\psi_{m,n}(t) = a_0^{-\frac{m}{2}}\psi(a_0^{-m}t - nb_0), \quad m, n \in \mathbb{Z} \tag{2.15}$$

The widely used DWT in signal processing applications is by discretizing the wavelet on dyadic time scale such that $a_0 = 2$ and $b_0 = 1$ that is called dyadic wavelet transform.

$$\psi_{m,n}(t) = 2^{m/2}\psi(2^{-m}t - n) \tag{2.16}$$

Where m and n denote scale and translation parameters respectively.

The DWT of a function f(t) hence becomes

$$\omega_f(m,n) = \langle f, \psi_{m,n} \rangle = \int_{-\infty}^{\infty} f(t)\psi^*_{m,n}(t)dt \quad (2.17)$$

The selection of *ψ(t)* is made such that the wavelet basis set *ψ{m,n}* constitute an orthonormal basis. Hence the wavelet expansion of *f (t)* can be expressed as

$$\hat{f}(t) = \sum_m \sum_n \omega_f(m,n)\Psi_{m,n}(t) \quad (2.18)$$

Equation (2.18) does not suffice PR and a portion of original signal is absent which will be dwelled in the subsequent sections. In the similar footing, we can extend discrete version of scaling function from (2.12) as follow

$$\varphi_{m,n}(t) = 2^{-\frac{m}{2}}\varphi(2^{-m}t - n) \quad (2.19)$$

Most of the signal energy is concentrated in fewer wavelet coefficients, therefore, it is also termed as sparse feature representation.

2.5 Multi resolution Analysis

MRA presents a systematic approach to generate the wavelets. The idea of MRA is to approximate a function *f(t)* at different levels of resolution. Two functions are considered: the mother wavelet *ψ(t)* and the scaling function *φ(t).* The scaled and translated versions of scaling function are given by (2.19). For fixed m, the set of scaling functions *φm,n(t)* are orthonormal. MRA is based on hierarchy of increasing resolutions of scaling functions and the wavelet functions emerge as consequence. By linear combinations of the scaling function and its translations we can generate a set of functions to represent any signal

$$f(t) = \sum_n \alpha_n \varphi_{m,n}(t), f(t) \epsilon V_m \quad (2.20)$$

The set [8] of all such functions generated by linear combinations of the set*{φm,n(t)}* is called span of the set, denoted by Span*{φm,n(t)}.* Now consider *Vm* to be vector space corresponding to the given set. Assume that the resolution increases with increasing *m*, these vector spaces describe successive approximation vector spaces

$V-\infty \subset \cdots \subset V-3 \subset V-2 \subset V-1 \subset V0 \subset V1 \subset V2 \subset V3 \subset \cdots \subset V\infty$

each with resolution 2^m. Similarly

$\cdots \perp W-3 \perp W-2 \perp W-1 \perp W0 \perp W1 \perp W2 \perp W3 \perp \cdots$ (2.21)

The set of subspaces must meet the following criteria in order to be a successful candidate for MRA

a. Each space must be contained in the next higher resolution space

$$V_m \subset V_{m+1} \cdots \forall m \in \mathbb{R} \quad (2.22)$$

b. b. The union of subspaces is dense in the space of square integrable functions $L^2(\Re)$

$$\overline{UV_m} = L^2(\Re) \tag{2.23}$$

c. The intersection of all the spaces is a singleton set containing the all zero function or zero vector

$$\overline{\cap V_m} = 0 \tag{2.24}$$

d. Contracting a function from resolution space V_0 by a factor of 2^m results in the higher resolution space V_m

$$f(t) \in V_o \leftrightarrow f(2^m t) \in V_{m.....m} \ \in \ \mathbb{R}^+$$

Or if

$$f(t) \in V_m \leftrightarrow f(2^p t) \in V_{m+p} \ldots . m, p \ \in \ \mathbb{R}^+ \tag{2.25}$$

e. The spaces are shift invariant i.e. translating a function in a resolution space does not change the resolution

$$f(t) \in V_o \leftrightarrow f(t-n) \in V_o \tag{2.26}$$

f. There exist a set that its integer translates forms an orthonormal basis of V_o

$$\{\varphi(t-n) \in V_o : n \ \in \ \mathbb{Z}\}$$

such that

$$\langle \varphi_m, \varphi_n \rangle = \partial\partial_{mn} = \{^{0 \ m \neq n}_{1 \ m=n} \tag{2.27}$$

The doctrine of MRA is that lower dimensional signals can be elegantly represented in higher dimensional spaces. As the spaces are nested within the next higher dimensional space, so the difference between the two adjacent spaces is the orthogonal complement of the lower dimension space within the next higher dimensional space i.e.

$$\langle \varphi_{m,n}, \Psi_{m,k} \rangle = 0 \ldots . . \forall \ m, n, k \ \in \mathbb{Z} \tag{2.28}$$

For a space $V_m$along its orthogonal complement say W_m, will constitute the next higher dimensional space V_{m+1}

$$V_{m+1} = V_m \oplus W_m \tag{2.30}$$

or equivalently

$$V_m = V_{m-1} \oplus W_{m-1} \tag{2.29}$$

which can be further decomposed into lower dimensional spaces along with their complements

$$V_m = V_{m-2} \oplus W_{m-2} \oplus W_{m-1}$$
$$= V_{m-3} \oplus W_{m-3} \oplus W_{m-2} \oplus W_{m-1} \quad (2.31)$$

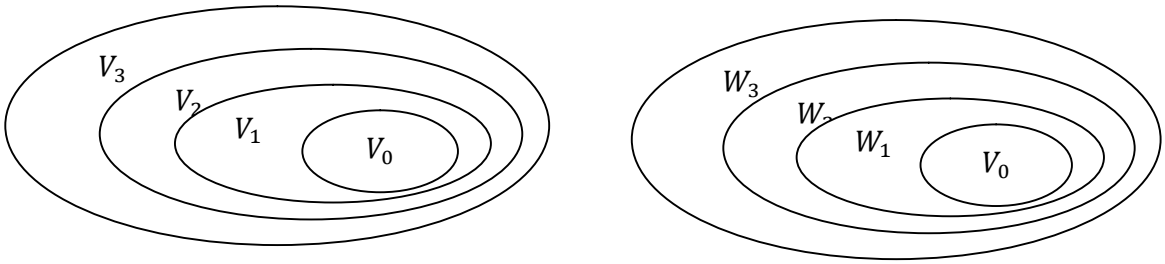

Figure 2.1 Nested spaces. (a) Nested function spaces spanned by scaling functions (b) Relation between scaling and wavelet spaces

We can express space of all the measureable and square integral functions as

$$\mathcal{L}^2(\Re) = V_0 \oplus \sum_{M=0}^{\infty} W_m = V_k \oplus \sum_{p \geq k}^{\infty} W_p \quad (2.32)$$

or even

$$\mathcal{L}^2(\Re) = \sum_{M=-\infty}^{\infty} W_m \quad (2.33)$$

As per above description of spaces, it is prudent to say that

$$\varphi(t) \in V_o \Leftrightarrow \varphi(2t) \in V_1 \quad (2.34)$$

which ensures elements in a space are simply scaled versions of the elements in the next space and if *φ(t)* is in *Vo* it is also in *V1* spanned by the spaceφ(2t). *Vo* and *Wo* are the subspaces of *V1* which can be expressed in terms of dilation equations or refinement relations for Haar

$$\varphi\ (t) = \varphi\ (2t) + (2t - 1) \quad (2.35)$$

Similarly

$$\psi\ t = \varphi\ 2t - (2t - 1) \quad (2.36)$$

In general φ(t) can be expressed in terms of weighted sum of shifted *φ(2t)* as

$$\varphi(t) = \sum_n h_\emptyset(n)\sqrt{2}\varphi(2t-n) \ldots\ldots n \in \mathbb{Z} \tag{2.37}$$

$\sqrt{2}$ is normalization constant, with similar reasoning and supplemented with Figure 2.1, we find that the wavelets too reside in the space spanned by the next narrower scaling function and can be represented by a weighted sum of shifted scaling functions

$$\psi(t) = \sum_n h_\varphi(n)\sqrt{2}\varphi(2t-n) \ldots\ldots n \in \mathbb{Z} \tag{2.38}$$

Equation (2.38) establishes that wavelets span the orthogonal complement spaces and integer shifts are also orthogonal, therefore relation between h_φ is inverted and modulated form of h_ψ that can be stated as

$$h_\varphi(n) = (-1)^n h_\varphi(1-n) \tag{2.39}$$

So far we developed the concept of nested spaces by which any finite energy signal in space can be represented by linear combination of bases from its subspace along its orthogonal complements. If $f_{m+1}(t)$ has the resolution *m+1* then it can be expanded as

$$f_{m+1}(t) = \sum_n \propto_{m,n} \varphi_{m,n} + \sum_n \beta_m \psi_{m,n} \tag{2.40}$$

Incorporating (2.37) and (2.38) in (2.40) we can represent a function *f(t)*$\in V_0$ as

$$f(t) = \sum_n h_\varphi(n)\sqrt{2}\,\varphi(2t-n) + \sum_n h_\psi(n)\sqrt{2}\,\varphi(2t-n) \tag{2.41}$$

Equation (3.41) represents the complete V_o space in the form of its scaled and translated versions of the next higher space. Thus a signal *f(t)* can be expanded in general as

$$f(t) = \sum_{m,n\in\mathbb{Z}} \langle f, \psi_{m,n}\rangle\, \psi_{m,n}(t) \tag{2.42}$$

$$= \sum_{n\in\mathbb{Z}} \langle f, \varphi_{m,n}\rangle \varphi_{m,n}(t) + \sum_{K\le m,n\in\mathbb{Z}} \langle f, \psi_{k,n}\rangle \varphi_{k,n}(t)$$

or can be stated as

$$f(t) = \sum_k \propto_{j_0}(k)\varphi_{j_{0,k}}(t) + \sum_{j=j_0}^{\infty}\sum_k \beta_{j_k}(k)\psi_{j_{,k}}(t), j_0 \ge k \tag{2.43}$$

Where j_0 is an arbitrary starting scale and $a_{j0}(k)$ and $\beta_j(k)$ are called .approximation and detail coefficients respectively which are obtained by taking the inner products of the function with scaling and wavelet functions as following

$$a_{j0}(k) = \langle f, \varphi_{j0,k} \rangle = \int f(t)\varphi_{j_{0,k}}(t)dt \tag{2.44}$$

$$\beta_j(k) = \langle f, \psi_{j0,k} \rangle = \int f(t)\psi_{j_{0,k}}(t)dt \tag{2.45}$$

Equation (2.43) also called wavelet expansion series, reconstructs the original signal without noticeable error and incorporates the lost portion of *f(t)* that was missing in (2.18).

2.6 Implementation of Wavelets

2.6.1 Image Pyramids

A lot of similarities have been found between MRA equations and image pyramids in which image is decomposed into its lower resolutions making pyramid like image structure [9]-[10] as shown in figure 2.2. Prediction residual is taken at each level so that its inverse transform exist without error. The Image pyramid along with prediction residual as depicted in figure is analogous to course scale approximations and fine scale details of the wavelets.

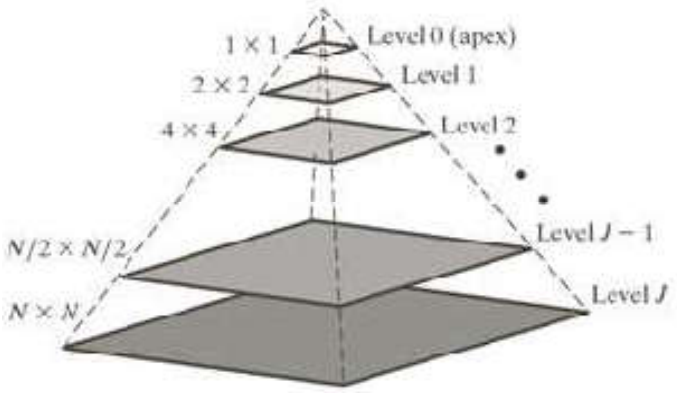

Figure 2.2 Image pyramid

2.6.2 Subband Coding

The wavelets could not be effectively implemented in signal processing applications till its linkage with subband coding was explored. In this scheme, the

image is decomposed into a set of band limited components, called subbands. The decomposition is performed in a manner such that the decomposed bands can be inverted back to re-construct the original signal without error. The decomposed signal is decimated such that it retains same number of data points after decimation as the original signal. Each decomposed band is separately up sampled and filtered in such a way that their combination yields back the original signal or in other words the combination of lower dimensional space can generate the next higher dimensional space. For this purpose; the transfer function of the system should be unity i.e. the synthesis filter bank should be the inverse of the analysis filter bank.

$$[L^T \;\; B^T]\begin{bmatrix} L \\ B \end{bmatrix} = I$$

$$\begin{bmatrix} L \\ B \end{bmatrix}[L^T \;\; B^T] = \begin{bmatrix} I & 0 \\ 0 & I \end{bmatrix} \tag{2.46}$$

Where L and B denote coefficients of analysis filter bank then their transpose constitute coefficients of synthesis filter bank.

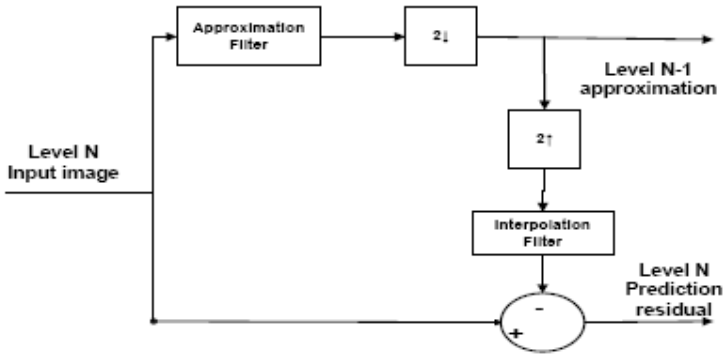

Figure 2.3 Pyramid Implementation

Another way to say is to factorize unity into two factors. One factor can correspond to coefficients of analysis filter bank and the other factor can correspond to synthesis filter bank. However these factors are constrained by certain mathematical conditions. There is no set procedure or derivations for finding these factors. The factors may be termed as magic numbers fulfilling the mathematical conditions such as compact support and orthogonality or biorthogonality in order to be successful candidate for wavelets.

Consider two channel perfect reconstruction filter bank as shown in Figure 2.4. The analysis filter bank consists of $h_o[n]$ and $h_1[n]$, is used to break the input sequence *f[n]* into two half length sequence $h_{lp}[n]$ and $h_{hp}[n]$, the subbands that represents

the input. The *ho[n]* and *h1[n]* are half band filters whose idealized transfer characteristics, h_o and h_1 are shown in figure 2.5 (b). Filter $h_o[n]$ is a lowpass filter whose output, subband $f_{lp}[n]$, is called an approximation of *f[n]* while $h_1[n]$ is a high pass filter whose output, subband $f_{hp}[n]$, is called high frequency or detail part of *f[n].* These filters are power complementary and FIR Each band is decimated by of two so that the amount of data should coincide with original signal. For synthesis the signal is up sampled by a factor of two by inserting zeros in between consecutive samples. Then it is passed to synthesis filters separately and then combined to re-construct the signal.

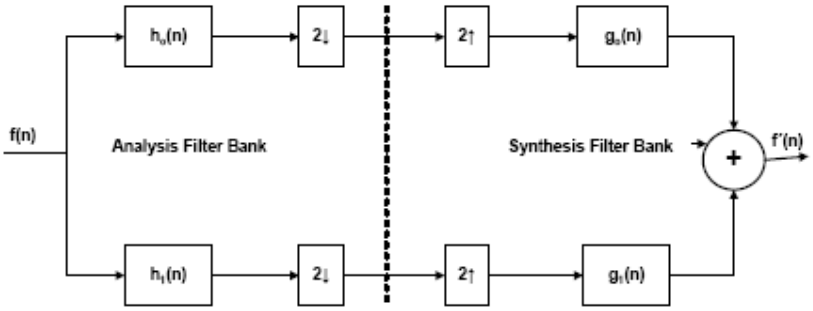

Figure 2.4 Subband coding and synthesis filter bank

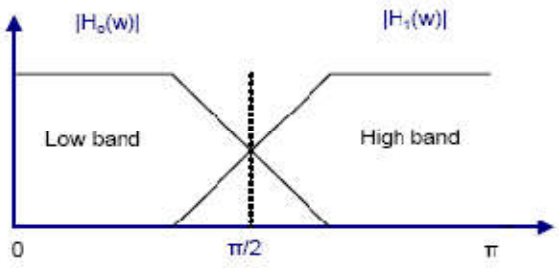

Figure 2.5 Spectrum of half band filters

The goal in subband coding is to select $h_o[n]$, $h_1[n]$, $g_o[n]$ *and* $g_1[n]$ so that $f\acute{[}n] = f[n]$.That is to say that input and output of subband coding and decoding system are identical.

In all sub band coding, synthesis filters are modulated version of the analysis filters. One synthesis filter is being reversed as well. For perfect reconstruction, the impulse responses of the synthesis and analysis filters must be related in one of the following form

$$g_0[n] = (-1)^n h_1[n] \tag{2.47}$$

$$g_1[n] = (-1)^{n+1} h_0[n] \tag{2.48}$$

or

$$g_0[n] = (-1)^{n+1} h_1[n] \tag{2.49}$$

$$g_1[n] = (-1)^{n} h_0[n] \tag{2.50}$$

Filter $h_o[n], h_1[n], g_o[n]$ *and* $g_1[n]$ in above equations are said to be cross modulated because diagonally opposed filters in Figure 2.4 are related by modulation. Further that, they satisfy the under mentioned biorthogonal condition

$$\langle h_i[2^n - k], g_j[k] \rangle = \partial[i-j]\partial[n], i, j = \{0,1\} \tag{2.51}$$

To develop fast wavelet transform we put further constrains such that

$$\langle g_i[2^n - k], g_j[n + 2m] \rangle = \partial[i-j]\partial[n], i, j = \{0,1\} \tag{2.52}$$

which defines orthonormality for perfect reconstruction filter banks. In addition to equation above, orthonormal filters can be shown to satisfy the following two conditions

$$g_1[n] = (-1)^n \, g_0 \, [k_e - 1 - n] \tag{2.53}$$

$$h_i[n] = \, g_i \, [k_e - 1 - n] \, , i, j = \, \{0,1\} \tag{2.54}$$

where the subscript k_e is used to indicate that the number of filter coefficients must be even. Above equations indicate that synthesis filter g_1 is related to g_0 by order reversal and modulation. In addition both h_1 and h_0 are order reversed version of synthesis filters g_1 and g_0. Thus an orthonormal filter bank can be developed around an impulse response of a single filter, called prototype, the remaining filters can be computed by using (2.47)- (2.54). Subband coding in the similar fashion can be applied to two dimension separable signals by processing in one dimension followed by the other dimension which will be discussed in the next sections.

2.6.3 Fast wavelet Transform

The wavelets could not be effectively used till Mallat [11] discovered that continuous wavelet basis formed by inner products of orthonormal basis can be implemented by a band of constant *Q* filters, the non overlapping bandwidths of which differ by an octave. A lot of similarities have been found in FWT and subband coding. The highpass $h_1[n]$ and lowpass $h_0[n]$ used in figure 2.4 for subband coding

have been used interchangeably as $h_\psi[n]$and $h_\varphi[n]$ respectively for clarity where needed without the loss of generality in the wavelet implementation through filter banks. Reconsider (2.37), scaling t by *2j* , translating by *k*, and substituting *m=2k+n*

$$\varphi(2^j x - k) = \sum_n h_\varphi\,[n]\sqrt{2}\varphi\big[2(2^j x - k) - n\big]$$

$$= \sum_m h_\varphi\,[m - 2k]\sqrt{2}\;\varphi\big[2^{j+1}x - m\big] \tag{2.55}$$

The scaling vector h_φ can be thought of as the weights used to expand $\varphi(2^j x - k)$ as sum of scale *j+1* scaling functions. A similar sequence of operations on (2.38) yields

$$\psi(2^j x - k) = \sum_m h_\varphi\,[m - 2k]\sqrt{2}\;\varphi\big[2^{j+1}x - m\big] \tag{2.56}$$

Putting the value of $\psi(2^j x - k)$ in (2.45) results

$$\beta_j(k) = \int f(t)2^{j/2}\left[\sum_m h_\psi[m - 2k]\sqrt{2}\varphi\big[2^{j+1}x - m\big]\right]dx$$

With a little manipulation of integrals and summation we get

$$\beta_j(k) = \sum_m h_\varphi\,[m - 2k]\left[\int f(t)2^{(j+1)/2}\,\varphi\big[2^{j+1}x - m\big]\right]dx \tag{2.57}$$

Therefore, the above equation can be written as

$$\beta_j(k) = \sum_m h_\varphi[m - 2k]\;\propto_{j+1}(m) \tag{2.58}$$

The detail coefficients at scale *j* are functions of the approximation coefficients at scale *j+1*. In similar fashion the wavelet series expansion approximation coefficients yield

$$\propto_j(k) = \sum_m h_\varphi[m - 2k]\;\propto_{j+1}(m) \tag{2.59}$$

When f(t) is discrete, the wavelet series expansion coefficients become DWT coefficients $W_\psi(j,k)$ and $W_\varphi(j,k)$ which can be expanded showing relation between DWT coefficients with adjacent scales.

$$W_\psi(j,k) = \sum_m h_\varphi[m - 2k]W_\psi(j+1,k) \tag{2.60}$$

$$W_\varphi(j,k) = \sum_m h_\varphi[m-2k]W_\varphi(j+1,k) \tag{2.61}$$

Equation(2.58) and (2.59) reveals that higher dimensional signal can be decomposed into lower dimensional signal. The scale and detail coefficients of higher dimensional space can be calculated by order reversed scaling and wavelet vectors $h_\psi[n]$and $h_\varphi[n]$ and then decimation by two is similar to analysis bank as depicted in figure 2.6 with addition that $h_\psi[n] = h_\psi[-n]$and $h_\varphi[n] = h_\varphi[-n]$.

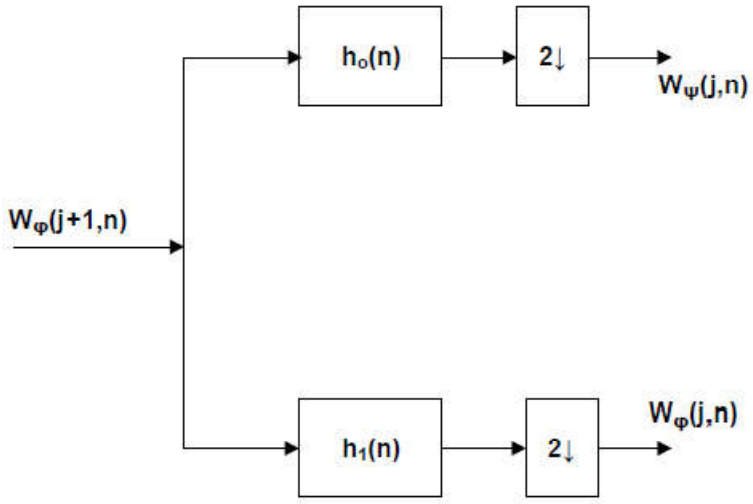

Figure 2.6 FWT analysis filter bank

Or can be equated as convolutions of $W_\varphi(j+1)$ with $h_\psi[n]$and $h_\varphi[n]$and then decimated by a factor of two yields

$$W_\psi(j,k) = h_\psi[-n] * W_\varphi(j+1,n)\big|_{n=2k,n} \tag{2.62}$$

$$W_\varphi(j,k) = h_\varphi[-n] * W_\varphi(j+1,n)\big|_{n=2k,n} \tag{2.63}$$

Above equations are the defining equations of FWT. The filter banks shown in preceding diagram can be iterated to yield multistage structures for computing DWT coefficients at two or more successive scales.

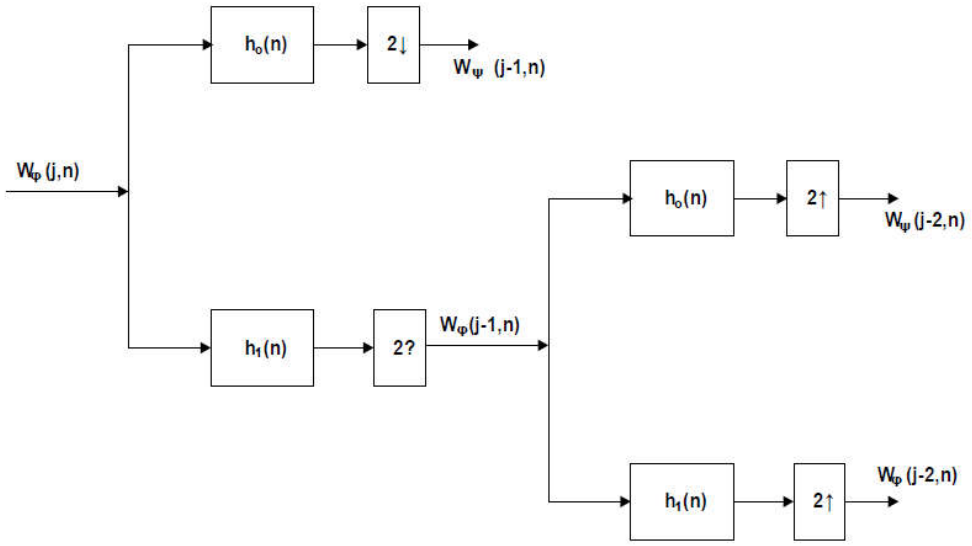

Figure 2.7 Two dimensional four band filter bank for suband coding

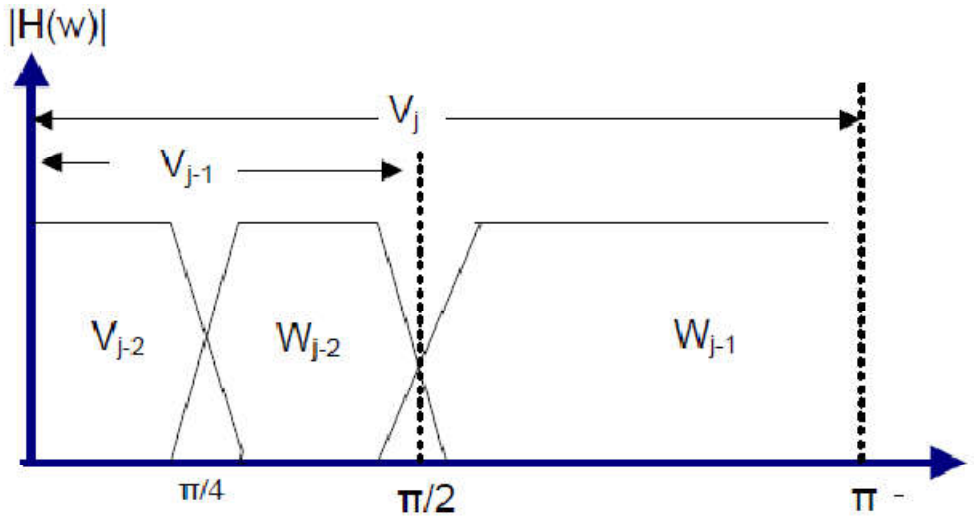

Figure 2.8 Spectrum splitting of the bands

The above diagram shows the iteration of $W_{\varphi}(j)$ *splitting to next resolution into* $W_{\psi}(j-1)$ *and*$W_{\varphi}(j-1)$. *The scaling function is again subjected to same lowpass and highpass filters yielding* $W_{\psi}(j-2)$ *and*$W_{\varphi}(j-2)$. Hence $W_{\varphi}(j-2)$ can further split into scaling and wavelet function in next lower dimension. The process can be iterated to any stage as per usage of the application. However the non-decomposition of data when it reaches to apex is trivial. The spectrum of the function as per their resolution is depicted in figure2.8.

The inverse wavelet transform is simple and the filter coefficients for inverse transform are calculated through (2.47)-(2.54). The scaling and wavelet vectors used in forward transform, together with level j approximation and detail coefficients generate the level j+1 approximation coefficients. The condition of order reversal of

filter coefficients must be taken into account for orthogonal filter banks. However for biorthogonal filter banks the analysis and synthesis filter should be cross modulated as per (2.53)- (2.54), which must be satisfied.

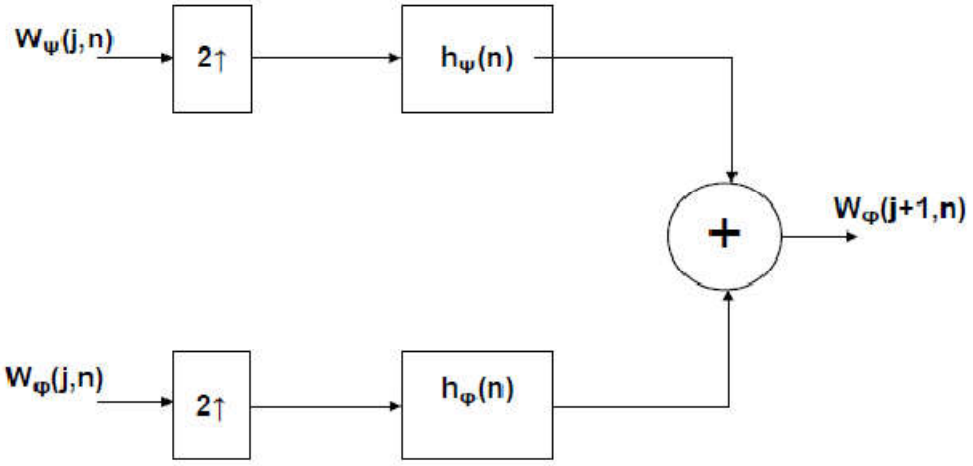

Figure 2-9 IFWT synthesis filter bank

The implementation of figure 2.9 can be worked out as

$$W_{\varphi}(j+1,k) = h_{\varphi}(k) * W_{\varphi}{}^{2\uparrow}(j,k) + h_{\varphi}(k) * W_{\varphi}{}^{2\uparrow}(j,k)\Big|_{k\geq o} \qquad (2.64)$$

where $\psi^{2\uparrow}$ signifies up sampling by two so that it gets back to original resolution. The up sampled coefficients are filtered with $h_{\psi}[n]$ and $h_{\varphi}[n]$ and then added to generate a higher scale approximation. The coefficients combining process as depicted in above figure can be extended upto any level provided the resolution is above single point. A two stage inverse FWT for Figure 3.7 is shown below which guarantees perfect construction.

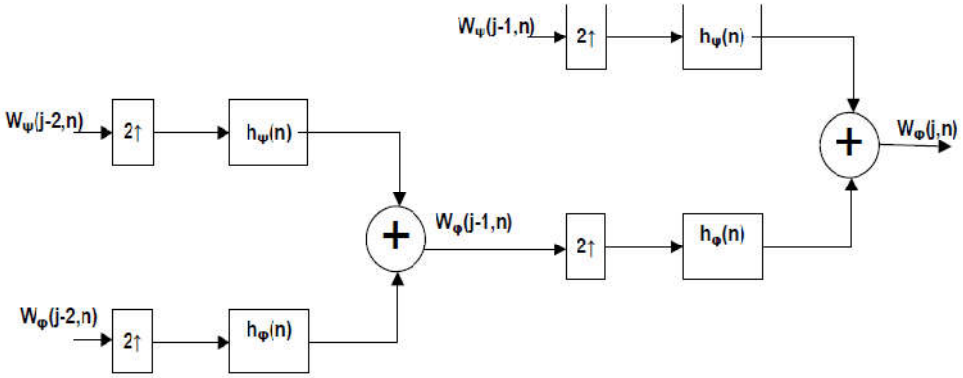

Figure 2.10 Two scale inverse IFWT synthesis filter bank

The existence of FWT depends upon the availability of a scaling function for the wavelets being used, as well as the orthogonality or bi orthogonality of the scaling function and corresponding wavelets. If these conditions are not met like Mexican

Hat wavelets which does not have a companion scaling function, cannot be implemented in filter banks.

In *Z* domain the conditions for perfect reconstruction [58], considering figure 2.4, can be established as

$$\widehat{F}(Z) = \frac{1}{2}G_o(Z)[H_o(Z)F(Z) - H_o(-Z)F(-Z)] + \frac{1}{2}G_1(Z)[H_1(Z)F(Z) - H_1(-Z)F(-Z)] \quad (2.65)$$

Rearranging the terms

$$\widehat{F}(Z) = \frac{1}{2}[H_o(Z)G_o(Z) - H_1(Z)G_1(Z)]\,F(Z) + \frac{1}{2}[H_o(-Z)G_o(Z) - H_1(-Z)G_1(Z)]F(-Z) \quad (2.66)$$

The above equations highlight the fact that for PR the aliasing effect due to down sampling and then up sampling, the filter responses must be such that these cancel the aliasing effects of each other i.e.

$$H_o(-Z)G_o(Z) - H_1(-Z)G_1(Z) = 0 \quad (2.67)$$

To eliminate the amplitude distortion effects, under mentioned must be satisfied

$$H_o(Z)G_o(Z) - H_1(Z)G_1(Z) = 2 \quad (2.68)$$

These equations can be simplified into matrix equations as

$$[G_o(Z)\ G_1(Z)]\begin{bmatrix} H_o(Z) & H_o(-Z) \\ H_o(Z) & H_o(-Z) \end{bmatrix} = [2\ 0] \quad (2.69)$$

Where analysis modulation matrix is

$$H_m(z) = \begin{bmatrix} H_o(Z) & H_o(-Z) \\ H_o(Z) & H_o(-Z) \end{bmatrix} \quad (2.70)$$

$$\begin{bmatrix} G_o(Z) \\ G_1(Z) \end{bmatrix} = \frac{2}{\det(H_m(Z))}\begin{bmatrix} H_1(-Z) \\ -H_0(-Z) \end{bmatrix} \quad (2.71)$$

The above matrix equation guarantees PR and the results are in line with the time domain analysis explaining orthogonality conditions in (2.47)-(2.52). Above equations can also demonstrate biorthogonality conditions by taking the product filter of lowpass and highpass as P (z)

$$P(z) = G_o(Z)H_o(Z) = \frac{2}{\det(H_m(Z))}\ H_o(Z)H_1(Z) \quad (2.72)$$

Similarly

$$G_1(Z)H_1(Z) = \frac{-2}{\det(H_m(Z))}H_o(-Z)H_1(Z) = P(-z) \quad (2.73)$$

or

$$G_1(Z)H_1(Z) = P(-z) = G_o(-Z)H_o(-Z) \tag{2.74}$$

Hence equations becomes

$$G_o(Z)H_o(Z) + G_o(-Z)H_o(-Z) = 2 \tag{2.75}$$

We can rewrite the equation after substituting the values

$$P(z) + P(-z) = 2 \tag{2.76}$$

Inverse *Zee* transform of (2.76) supplements the biorthogonality condition of the filters stated in (47)-(50) for PR of the original signal.

2.7 Wavelet's Extension in Higher Dimensions

One dimensional transform can be easily extended to two dimension provided [1] that the signal must be separable i.e. filtering and down sampling can be applied in one dimension followed by the other dimension. For images, a two dimensional scaling function φ(x, y) and three two dimensional wavelets, $\psi^1(x,y)$, $\psi^2(x,y)$ and $\psi^3(x,y)$ are required. Each function is the product of separable two one dimensional functions and separable directional wavelets.

$$\varphi(x,y) = \varphi(x)\varphi(y) \tag{2.77}$$

$$\psi^1(x,y) = \psi(x)\varphi(y) \tag{2.78}$$

$$\psi^2(x,y) = \varphi(x)\psi(y) \tag{2.79}$$

$$\psi^3(x,y) = \psi(x)\psi(y) \tag{2.80}$$

Equation (2.77) calculates the approximation and remaining equations calculate directional variations. Equations (2.78), (2.79) and (2.80) give variation along horizontal, vertical and diagonal directions respectively. Two dimensional wavelets can be simply extended from one dimensional wavelet as

$$\varphi_{j,m,n}(x,y) = 2^{j/2}\psi\left(2^j x - m, 2^j y - n\right) \tag{2.81}$$

$$\psi^i_{j,m,n}(x,y) = 2^{j/2}\psi^j\left(2^j x - m, 2^j y - n\right), i = 1,2\&3 \tag{2.82}$$

Where index *i=1,2,3* indicates the directional wavelets i.e. horizontal, vertical and diagonal. The DWT of image f(x,y) of size M x N is

$$W_\varphi(j_0,m,n) = \frac{1}{\sqrt{MN}}\sum_{X=0}^{M-1}\sum_{Y=0}^{N-1} f(x,y)\,\varphi_{j_0,m,n}(x,y) \tag{2.83}$$

$$W^i_\psi(j,m,n) = \frac{1}{\sqrt{MN}}\sum_{X=0}^{M-1}\sum_{Y=0}^{N-1} f(x,y)\,W^j_{i,m,n}(x,y)\,, i = \{H,V,D\} \tag{2.84}$$

As in one dimensional case, j_0 is an arbitrary starting scale and $W_\varphi(j_0,m,n)$ coefficients define an approximation of f(x,y) at scale j_0. The $W_\psi^i(j,m,n)$ coefficients add horizontal, vertical and diagonal details for scales j ≥ j_0.Normally j_0=0 and N=M=2^j for j=0,1,2,3…, j-1 and m=n= 0,1,2,…, 2^{j-1} is taken.

The inverse two dimensional DWT can be obtained by

$$f(x,y)=\frac{1}{\sqrt{MN}}\sum_{X=0}^{M-1}\sum_{Y=0}^{N-1}W_\varphi(j_0,m,n)\varphi_{j_0,m,n}(x,y)$$

$$+\frac{1}{\sqrt{MN}}\sum_{i=H,V,D}\sum_{J=J_0}^{\propto}\sum_{m}\sum_{n}W_\psi^i(j,m,n)\ \psi_{j,m,n}^i(x,y) \qquad (2.85)$$

Two dimensional separable scaling and wavelet functions can be implemented by simply taking the one dimensional FWT of the rows of f(x,y) followed by one dimensional FWT of the resulting columns. Figure 2.11 shows the block diagram of the filter banks.

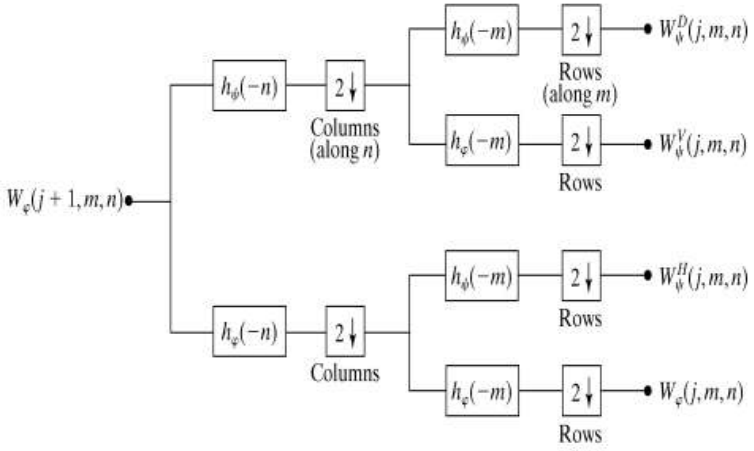

Figure 2.11 Two dimensional FWT; analysis filter bank using QMF for image decomposition

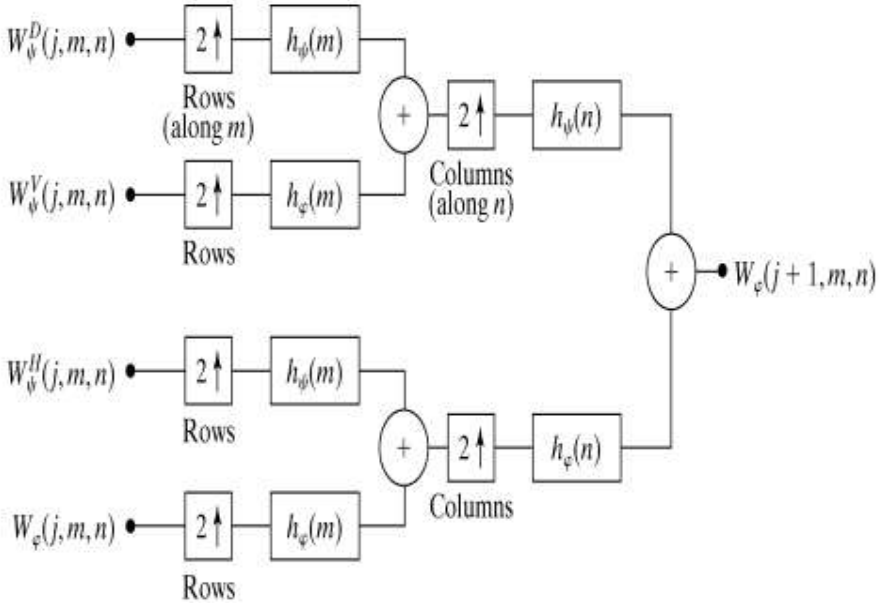

Figure 2.12 Image Synthesis using inverse QMF

CHAPTER 3

RIGOROUS EASY PATH WAVELET TRANSFORM (EPWT)

3.1. Introduction

Most methods for image compression were the tensor product image compression techniques which had a disadvantage of giving a particular importance to the horizontal and vertical directions. Tensor product orthogonal wavelet bases are unable to adapt towards directional geometric features. Consequently a lot of research to overcome this difficulty lead to adaptive wavelet transforms. Bandelets [13], Wedgelets [14], Tetrolets [15], Grouplets [16], are some of the main highlights of these adaptive techniques. This chapter presents a scheme for exploitation of correlated image pixels and moving on from neighbour to neighbour of each pixel value thereby finding a path vector across all points. Dyadic wavelet transform on the path vector is then used to produce coefficients for the next lower level images of high pass and low pass coefficients. However to achieve optimality of image compression level of image decomposition through wavelet transform is continued until a single pixel images are obtained. It is an extension to technique proposed by Naqvi [17].

Basic Terminologies

Let consider an image of even dimensions such that P and Q denote the dimensions and $\mathrm{PQ} = 2^{\mathrm{L}}\ \mathrm{P}, \mathrm{Q}, \mathrm{L} \in\ \mathbb{N}$. (p, q) can be indexed as $\mathrm{I} = \{(\mathrm{p}, \mathrm{q}) : \mathrm{p} = 0, \dots, \mathrm{P} - 1, \mathrm{q} = 0, \dots, \mathrm{Q} - 1\}$. A function 'S' that converts image indices to discrete sequence of numbers is such that:

$\mathrm{S}:\ \mathrm{I} \rightarrow \{0,1, \dots, (\mathrm{PQ} - 1)\}$, where $\mathrm{S}\big((\mathrm{p}, \mathrm{q})\big) := \mathrm{p} + \mathrm{qP}$.

If $(\mathrm{p}_1, \mathrm{q}_1) \in \mathrm{I}$, then the neighborhood, $\widetilde{\mathrm{nb}}$, of an index (p, q) is defined by:

$$\widetilde{\mathrm{nb}}(\mathrm{p}, \mathrm{q}) = \widetilde{\mathrm{nb}}(\mathrm{i}) = \{|\mathrm{p} - \mathrm{p}_1| \leq 1, |\mathrm{q} - \mathrm{q}_1| \leq 1\ \} \qquad (3.1)$$

$$\mathrm{p} \neq \mathrm{p}_1, \mathrm{q} \neq \mathrm{q}_1$$

Using discrete sequence of values from $S(I)$ neighbourhood of any pixel $i \in S$ as eq. (3.1) is as follows:

$$\widetilde{nb}(i)$$

$$= \begin{cases} \partial_0 \rightarrow \{(i+P),(i+P+1),(i+1)\} \\ \partial_1 \rightarrow \begin{Bmatrix}(i+P),(i+P+1),(i+1),\\ (i-1),(i+P-1)\end{Bmatrix} \\ \partial_2 \rightarrow \{(i+P),(i-1),(i+P-1)\} \\ \partial_3 \rightarrow \begin{Bmatrix}(i+P),(i-P),(i-P-1),\\ (i-1),(i+P-1)\end{Bmatrix} \\ \partial_4 \rightarrow \{(i-P),(i-P-1),(i-1)\} \\ \partial_5 \rightarrow \begin{Bmatrix}(i+1),(i-P+1),(i-P),\\ (i-P-1),(i-1)\end{Bmatrix} \\ \partial_6 \rightarrow \{(i+1),(i-P+1),(i-P)\} \\ \partial_7 \rightarrow \begin{Bmatrix}(i+P),(i+P+1),(i+1),\\ (i-P+1),(i-P)\end{Bmatrix} \\ \partial_8 \rightarrow \begin{Bmatrix}(i+P),(i+P+1),(i+1),\\ (i-P),(i-P+1),\\ (i-P-1),(i-1),(i+P-1)\end{Bmatrix} \end{cases} \quad (3.2)$$

∂_0	∂_7	∂_6
∂_1	∂_8	∂_5
∂_2	∂_3	∂_4

Figure 3.1 Grouping of indexes with common neighbours

Therefore, indices belonging to block ∂_8 have maximum neighbors. Dividing the index set such that F= $\{S_1, S_2, S_{3,\dots}, S_v\}$ and intersection of any two subsets is an empty set, mathematically where $S_a \cap S_b = \emptyset$ and union of all sets gives the indexed set S such that $\cup_{a=1}^{v} S_a = S$. Also $S_a \in \widetilde{nb}(S_b)$, if there is at least one index from each set who are neighbors of each other i.e. $i \in \widetilde{nb}(i_1)$. Connect a path through the index set S(I) of the image block such that absolute difference is minimum and encode these path indices. The complete path vector p^L through $S(I)$ is an integer vector of length PQ composed of all indices of $S(I)$ in a certain order. The complete path vector of all levels will constitute L number of path vectors i.e. if $PQ = 2^4$ then complete path vector of all levels will constitute p^4, p^3, p^2, p^1. Furthermore functional values of each path vector are compressed using DWT. Whenever a pathway is closes on itself a new pathway is chosen and such transition is known as *interruption.*

3.2. Rigorous Easy Path Wavelet Transform

Introduction

Determine a path along the indices of $S(I)$ of image as discussed before. Starting from the matrix value of $c(p,q) = (0,0)$ or S(0,0)={0}. Next from $\widetilde{nb}(0)$ (neighbouring pixels) lookup a function value whose relative value is nearest to 'f (S (0, 0) =0)'. This neighbour $c(p,q) \in \widetilde{nb}(0)$ will be our new entry in the path vector set. Mathematically:

$$p^L(i+1) = \underset{a}{argmin}\{\left|c^L\left(p^L(i)\right) - c^L(a)\right| a \in \widetilde{nb}\left(p^L(i)\right) \quad (3.3)$$

Where $a \in \widetilde{nb}(0)$ which are unoccupied or not in the path vector or admissible. $c^L\left(p^L(i)\right)$ is the function value of current index set (i). $p^L(i+1)$ is chosen from these admissible neighbors and that fulfils eq. 3.3. Similarly scan along the values of the matrix and calculate a series of path vectors that belong to one dimensional index set 'S'. Equation 3.3 may not give a unique answer, for that case chose the direction which follows the momentum of the previous pathway or *favorite direction*. Apart from the case of index when i= {0} one may come across a situation when no neighboring indices are empty and are already consumed in the pathway then start new pathway with preferably the smallest index left in the grid which reduces the computation complexity. Such situation is known as an interruption i.e. choose minimum available unused index in $S(I)$ as $p^L(i+1)$. Or another choice is to look for a next index, such that again the absolute difference is given by $\left|c^L\left(p^L(i)\right) - c^L(a)\right| a \in S(I)$ is minimal. After calculation of pathway, apply DWT using any dyadic wavelet, say e.g. Haar wavelets, along the pathway of values.

Lets take an example of two 4x4 matrices to delineate the concept of above mentioned technique of finding a path across all the data points of a image/frame. Suppose each frame is of dimensions *4 × 4* with following intensity values:

$$c^4 = \begin{bmatrix} 0.443 & 0.493 & 0.424 & 0.422 \\ 0.442 & 0.474 & 0.463 & 0.429 \\ 0.432 & 0.443 & 0.422 & 0.436 \\ 0.441 & 0.442 & 0.475 & 0.464 \end{bmatrix}$$

$$c^4 = \begin{bmatrix} 0.443 & 0.494 & 0.432 & 0.439 \\ 0.472 & 0.443 & 0.468 & 0.490 \\ 0.498 & 0.412 & 0.442 & 0.434 \\ 0.463 & 0.442 & 0.433 & 0.455 \end{bmatrix}$$

Let's walk through the indices of c^4 and find values that satisfy eq. (3.3). Initializing from $c^4(0.0) = 0.443$. Looking through the neighbors of $c^4(0.0) = 0.443$ i.e. $\widetilde{nb}(0)$

and finding an index that qualifies eq. 3.3. Following the above procedure which gives following first path vector:

$$p^4 = (0, 1, 6, 7, 3, 2, 5, 9, 14, 13, 8, 12, |4, | 10, 15, 11)$$

Where '|' signifies an interruption in the path vector.

Efficient Storage of Path Vector Set

To reduce the processing cost an efficient method is devised to reduce processing cost. We encode the path followed under eq. 3.3 instead of the indexed set sequence. Therefore a considerable budget is economized in shape of encoded path vector $\tilde{p}$. For first entry $p^L(0) = 0$ the encoded index is will be represented by $\tilde{p}^L(0) = 0$. This will always be used as a starting point. In future path vector entries, an entry will only be zero if it does not cause a change in pathway with respect to the previous pathway. This is known as following favorite direction. To encode the second entry $p^L(1)$ we follow a simple standard, put

$$\tilde{p}^L(1) = \begin{cases} 0 \; if \; p^L(1) = P \\ 1 \; if \; p^L(1) = P + 1 \\ 2 \; if \; p^L(1) = 1 \end{cases} \quad (3.3.1)$$

For encoding index values of the path vector we determine the favorite direction by the following equation:

$$p^L(i+1) = 2p^L(i) - p^L(i-1)) \quad (3.4)$$

If it is satisfied we put $\tilde{p}^L(i+1) = 0$. If the pathway does not satisfy eq. 3.4 then it means favorite direction is not followed and then it will be encoded with respect to right handed or clockwise distance. Mathematically consider the following set:

$$q = \left(q(\mu)\right)_{\mu=0}^{7} \in \mathbb{Z}^8 \quad (3.5)$$

and $q = (P, P+1, 1, -P+1, -P, -P-1, -1, P-1)$

Find the index $\tilde{\mu} \in \{0,1 \ldots 7\}$ which will direct towards the favorite direction such that

$$q(\tilde{u}) = (p^L(i) - p^L(i-1) \quad (3.6)$$

If there is a circular shift $\tilde{q}$ of q such that $\tilde{q} = q(\tilde{u}), \ldots q(7), q(0), \ldots \ldots . q(\tilde{u} - 1)$= $(\tilde{q}(\mu))_{\mu=0}^{7}$ and $\tilde{q}(0) = \tilde{q}(\mu)$. Above procedure gives us all possible neighbors with following encoded path vectors:

$$\tilde{p}^L(i+1) = \begin{cases} 0 & p^L(i+1) = p^L(i) + \tilde{q}(0) \\ 1 & p^L(i+1) = p^L(i) + \tilde{q}(1) \\ 2 & p^L(i+1) = p^L(i) + \tilde{q}(2) \\ 3 & p^L(i+1) = p^L(i) + \tilde{q}(3) \\ 4 & p^L(i+1) = p^L(i) + \tilde{q}(5) \\ 5 & p^L(i+1) = p^L(i) + \tilde{q}(6) \\ 6 & p^L(i+1) = p^L(i) + \tilde{q}(7) \end{cases} \quad (3.7)$$

If $\widetilde{nb}\left(p^L(i)\right)$ are not all admissible, we delete all components $\tilde{q}(\mu)\,\text{in}\,\tilde{q}$ that do not point towards and admissible neighbor (index) and follow the above procedure without changing the order.

For example encoding the third path vector i.e. index '6' the above mentioned procedure is as follows:

$q = (4, 5, 1, -3, -4, -5, -1, 3)$ then $q(\tilde{u}) = 1 - 0 = 1$ therefore giving a cyclic shift yields $\tilde{q} = \{1, -3, -4, -5, -1, 3, 4, 5\}$ which sets corresponding favorite direction as index '2' and following clockwise order and deleting non-admissible neighbors $\tilde{q} = \{1, 3, 4\}$ which means index '6' can be reached from index '1' when we add 4 into it. As $\tilde{q}(0) = 1$, so $\tilde{q}(3) = 4$ which upon using eq. 3.7 encodes '6' as '3'. Encoded pathway p^4 is:

$\tilde{p}^4 = (0,2,3,1,0,0,0,1,1,3,1,0, |0, |0,0,0)$

Presence of zero symbols signifies a sparser representation which means less space is engaged. Path vectors can be encoded more sparsely if Relaxed EPWT algorithm (described in later chapter) is used. When the path vectors are calculated a one dimensional discrete Haar wavelet transform on functional values $(c^L(p^L(i)))_{i=0}^{PQ-1}$ along all levels of path vectors is applied, which gives scaling function coefficients$c^{L-1} \in \mathbb{R}^{PQ/2}$, and a wavelet function coefficient $g^{L-1} \in \mathbb{R}^{PQ/2}$. Used filters are Haar filters such that $h(0) = h(1) = 1/2$ and $g(0) = -1/2$, $g(1) = 1/2$:

$$g^3 = (0.0005, 0.0005, 0.0045, 0.0055, 0.0035, 0.0010, 0.0355, -0.0055)$$

$$c^3 = (0.4425, 0.4425, 0.4365, 0.4685, 0.4325, 0.4230, 0.4575, 0.4695)$$

Subsequent Levels

As Haar wavelets decrease the size of the image at dyadic scale. Therefore we use interpolation to fill in the coefficients values that maintains the same size of

c^{L-1} as the original frame size c^L. Such interpolation yields a smooth continuous function $\tilde{c}^{L-1}$. So imitate the eight coefficients to produce 16 values. Such matrix or blown up version is obtained when each coefficient from low pass filtering is interpolated at the same index the path vector was calculated to getc^{L-1}. Mathematically:

$$S_i^{L-1} = \{p^L(2i), p^L(2i+1)\}, \text{where } i = 0, , \frac{PQ}{2} - 1 \quad (3.8)$$

As a result:

$$\tilde{c}^{L-1}\left(p^L(2i)\right) = c^{L-1}(i)\,; c^{L-1}\left(p^L(2i+1)\right) = c^{L-1}(i) \quad (3.9)$$

where $i = 0, \dots , \frac{PQ}{2} - 1$ .Thus we group all indices to retain the original size of matrix as PQ (4 x 4 here) and both indices grouped together are considered to be a single index for subsequent compression.

By above procedure c^3 takes form of $\widetilde{c^3}$:

$$\widetilde{c^3} = \begin{bmatrix} 0.4425 & 0.4575 & 0.4230 & 0.4230 \\ 0.4425 & 0.4685 & 0.4685 & 0.4325 \\ 0.4365 & 0.4425 & 0.4575 & 0.4325 \\ 0.4365 & 0.4425 & 0.4695 & 0.4695 \end{bmatrix}$$

First member of each c^L will always be considered as index '0'. For further evaluation of path vector indices, $p^{L-j}(i+1)$, if present entry is $p^{L-j}(i)$, apply the following equation for $0 < j < L$:

$$p^{L-j}(i+1) = \underset{a}{\operatorname{argmin}} \left\{ \left| c^{L-j}\left(p^{L-j}(i)\right) - f^{L-j}(a) \right| \right\} \quad (3.10)$$

Where $f^{L-j}(a)$ are the function values of the neighboring index set 'a'. More generally evaluation of neighboring index sets of S_i^{L-j} where $0 < j < L$ is:$\widetilde{nb}\left(S_i^{L-j}\right) =$

$$\widetilde{nb}\left(S^{L-j+1}_{p^{L-j+1}(2i)}\right) \cup \widetilde{nb}\left(S^{L-j+1}_{p^{L-j+1}(2i+1)}\right) \quad (3.11)$$

As before again DWT using Haar is operated on the path vectors. Applying above equations result in following:

$p^3 = (0,1,2,3,6,7,4,5)$

$\tilde{p}^3 = (0,1,1,0,1,1,0,0)$

$c^2 = (0.4425, 0.4525, 0.4635, 0.4277)$

$g^2 = (0, -0.0160, 0.0047, -0.0060)$

$0.5575, 0.5695)$

$\widetilde{c^2}$ is obtained by interpolation:

$$\widetilde{c^2} = \begin{bmatrix} 0.4425 & 0.4635 & 0.4277 & 0.4277 \\ 0.4425 & 0.4525 & 0.4525 & 0.4277 \\ 0.4525 & 0.4425 & 0.4635 & 0.4277 \\ 0.4525 & 0.4425 & 0.4635 & 0.4635 \end{bmatrix}$$

And next path vector with its encoded counterpart is:

$p^2 = (0,1,2,3)$

$\tilde{p}^2 = (0,0,1,0)$

Similarly for next level:

$c^1 = (0.4475, 0.4456)$

$g^1 = (-0.0050, -0.0179)$

Interpolation gives $\tilde{c}^1$:

$$\widetilde{c^1} = \begin{bmatrix} 0.4475 & 0.4456 & 0.4456 & 0.4456 \\ 0.4475 & 0.4475 & 0.4475 & 0.4456 \\ 0.4475 & 0.4475 & 0.4456 & 0.4456 \\ 0.4475 & 0.4475 & 0.4456 & 0.4456 \end{bmatrix}$$

Similarly path vector for this level is:

$p^1 = (0,1)$

$\tilde{p}^1 = (0,0)$

In the end a single scaling function coefficient and single wavelet function coefficient i.e.$c^0 = (0.4466),\ g^0 = (0.00095)$. Entropy is given as $\sum_m p_m \log_2 1/p_m$ where p_m is the probability of a symbol. Entropy of $\tilde{p}_1^4$ where $p_0 = \frac{9}{16}, p_1 = \frac{4}{16}, p_2 = \frac{1}{16}, p_3 = \frac{2}{16}$ is **1.591 bits per symbol or bits per pixel**. Applying similar procedure on 2nd image/frame c^4 :

$$c^4 = \begin{bmatrix} 0.443 & 0.494 & 0.432 & 0.439 \\ 0.472 & 0.443 & 0.468 & 0.490 \\ 0.498 & 0.412 & 0.442 & 0.434 \\ 0.463 & 0.442 & 0.433 & 0.455 \end{bmatrix}$$

For f= 2 & $L = 4$:

$p^4 = (0, 5, 10, 7, 11, 14, 15| 1, 4, 9, 13, 12, 8 | 2, 3, 6)$

$\tilde{p}^4 = (0, 1 ,0 ,2 ,3 ,1 ,0 | 0 ,0 ,1 ,3 ,1 ,0 | 0 ,1 ,0)$

$c^3 = (0.4430, 0.4420, 0.4335, 0.4635, 0.4810,\ 0.4645, 0.4650, 0.4375)$

$g^3 = (0, 0, -.0005, -.0085, .0130, 0.0255, -0.0330, .0255)$

Again we find a path vector as follows:

$p^3 = (0,1, 7, 2 , 3, 6, 5, 4)$

$\tilde{p}^3 = (0, 0, 5, 1, 0, 1, 0, 0)$

Applying wavelet filters we evaluate the coefficients as:

$c^2 = (0.4425, 0.4355, 0.4642, 0.4727)$

$g^2 = (0.0005, 0.0020, -0.0007, -0.0082)$

Again same procedure as applied:

$p^2 = (0,1,2,3)$

$\tilde{p}^2 = (0,0,0,0)$

Coefficients of this level are:

$c^1 = (0.4390, 0.4685)$

$g^1 = (0.0035, -0.0043)$

At the last level $p^1 = (0,1)$; $\tilde{p}^1 = (0,0)$; $C^0 = (0.4537)$; $g^0 = -0.0147$. Entropy of second frame at level four i.e $\tilde{p}^4$ as 1.69 bits per pixel.

All path vectors are requisite for perfect lossless reconstruction, therefore we store them separately.

Reconstruction Algorithm

Using the following code we can reconstruct back our original matrix of pixel values with the help of

$$p = (p^1, p^2, p^3, \dots, p^L) \in \mathbb{R}^{2PQ(1-\frac{1}{2^L})} \text{and } T = (c^0, g^0, g^1, \dots, g^{L-1}) \in \mathbb{R}^{PQ}$$

$$for\ (\boldsymbol{f} = 1, f \leq f, f++)$$

{ $for\ (j = 0, j \leq L-1, j++)$

{

Applying IDWT to the vector $\begin{pmatrix} c^j \\ g^j \end{pmatrix} \in \mathbb{R}^{2^j}$ to obtain c^{j+1}. c^{j+1} are restricted to their location by:

$$c^{j+1}\left(p^j(a)\right) = c^{j+1}(a), \text{where } a = 0, \dots, 2^{j+1} - 1$$

}

}

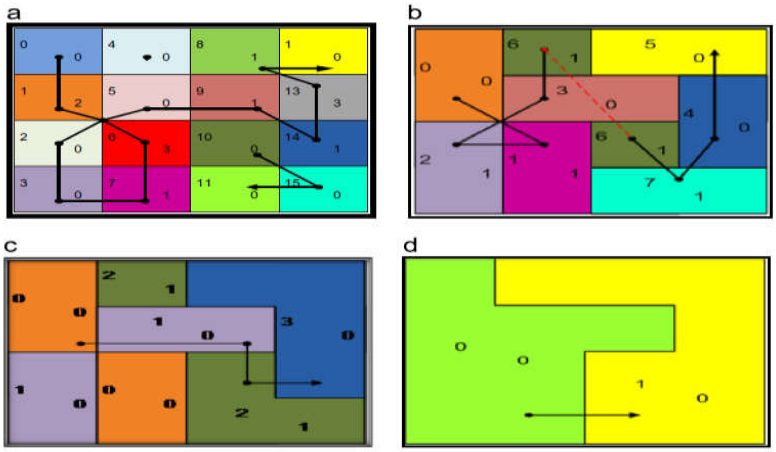

Figure 3.2 Pathways followed by Rigorous EPWT at (a) L= 4, (b) L= 3,(c) L= 2, (d) L= 1

CHAPTER 4

RELAXED EASY PATH WAVELET TRANSFORM (EPWT)

4.1. Relaxed EPWT

To decrease the computational complexity of Rigorous EPWT Relaxed EPWT can be employed where we a special bound '∅' is set and if this threshold is violated only then the direction of the pathway is changed otherwise it keeps on following the favorite direction which ensures encoded path vector to have maximum zeroes.

4.2. Calculation of Path Vector

Threshold criterion is set as follows and if it is satisfied a symbol '0' is encoded in the path vector :

$$\left|c^L\left(p^L(i)\right) - c^L\left(2p^L(i) - p^L(i-1)\right)\right| \leq \emptyset \quad (4.1)$$

$\left(2p^L(i) - p^L(i-1)\right)$ determines the favorite direction in eq. (4.1). If $(i-1) = 0\ and\ (i) = 4$ which is the favorite direction starting from '0' index then eq. 41 gives index '8'. This condition will not cater for any neighbors of index 'i' unless violated. If favorite direction is already occupied then use the condition employed in the previous section of Rigorous EPWT. We delete all components $\tilde{q}(\mu)\ \text{in}\ \tilde{q}$ that do not give an admissible index and the scheme will be altered as $\tilde{p}^L(i+1) := b\ ;\ if\ p^L(i+1) = p^L(i) + \widetilde{q(\mu)}$ and if the selected $p^L(i+1)$satisfies$\left|c^L\left(p^L(i)\right) - c^L\left(p^L(i)\right)\right| \leq \emptyset$. If equation above threshold fails to satisfy then we fall back to Rigorous EPWT to determine $p^L(i+1)$ which warrants us to use the following equation:

$$p^L(i+1) = \underset{a}{\text{argmin}}\left\{\left|c^L\left(p^L(i)\right) - f^L(p^L(a)\right|\right\} \quad (4.2)$$

It can be seen that all path vectors follow the favorite direction criteria as the threshold is not violated. This causes the encoded path vector $\tilde{p}^4$ have all zeroes in it which considerably reduces the overall entropy. Diagrammatically path vectors are shown in fig4.1 [a-d].

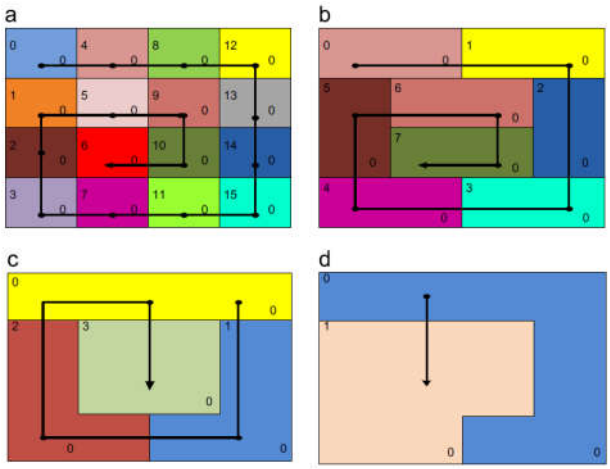

Figure 4.1 Relaxed EPWT pathways for $\phi = 0.1$ (a) L= 4, (b) L= 3,(c) L= 2, (d) L= 1

If set a threshold to be $\phi = 0.1$ then it will be violated almost every time and our Relaxed EPWT will be equivalent to Rigorous EPWT. It is of importance to note that as the size of the image increases the entropy of path vector cut down rapidly.

4.3. Further Levels

Converting the adjacent entries to a form a single index for further compression. After combining these entries DWT is taken and a blown up image is created by interpolating the matrix with scaling coefficient. As before first entry of path vector is always taken o be '0'. Therefore $\tilde{p}^{L-j} = 0$ is first member of encoded set. For determining subsequent path entries use the already index set or current index set 'i' from first level and proceed as follows for $i \geq 0$: If $p^{L-j}(i) + 1$ is an admissible neighbor of $p^{L-j}(i)$ and it fulfills the threshold criterion:

$$|c^{L-j}\left(p^{L-j}(i)\right) - c^{L-j}\left(p^{L-j}(i) + 1\right)| \leq \emptyset \qquad (4.3)$$

Then we can take it as our next path vector entry as

$p^{L-j}(i+1) := p^{L-j}(i) + 1$ and encode it as $\tilde{p}^{L-j}(i+1) := 0$. There may be a case when $p^{L-j}(i) + 1$ is not an admissible neighbor of $p^{L-j}(i)$ or it fails to satisfy eq. (4.4) then check on $p^{L-j}(i) - 1$ as the next candidate and similarly apply eq. (4.4) in following manner:

$$|c^{L-j}\left(p^{L-j}(i)\right) - c^{L-j}\left(p^{L-j}(i) - 1\right)| \leq \emptyset \qquad (4.4)$$

If the both conditions above satisfy then $p^{L-j}(i+1) := p^{L-j}(i) - 1$ and encoded entry is '0' if $p^{L-j}(i+1)$ not admissible neighbor of $p^{L-j}(i)$ and if it is then take encoded entry to be '1'.

If all above conditions fail to satisfy then look through all admissible neighbors in $\{0,1,\ldots\ldots,(\frac{PQ}{2^j}-1)\}$ of $p^{L-j}(i)$ and place them in a vector c^* in descending order of the index. Remove $p^{L-j}(i)+1$, $p^{L-j}(i)-1$ and let $i_o \in \{0,1,2\}$ be removed indices. Let $c^*(\alpha)=(c^*(0),c^*(1),c^*(2)\ldots)$ be the vector that contains the admissible neighbor of $p^{L-j}(i)$ then take α^* which is the smallest index of $c^*(\alpha)$, such that it qualifies the following equation:

$$|c^{L-j}\left(p^{L-j}(i)\right)-c^{L-j}(c^*(\alpha^*))|\leq \emptyset \tag{4.5}$$

If the above condition is satisfied then $p^{L-j}(i+1):=c^*(\alpha^*)$ and $\tilde{p}^{L-j}(i+1):=\alpha^*+i_0$. If still no above conditions fail to hold then look for neighbors of index $p^{L-j}(i)$ that gives minimum absolute difference value, mathematically:

$$\alpha^*=\underset{\alpha}{\operatorname{argmin}}\left\{\left|c^{L-j}\left(p^{L-j}(i)\right)-c^{L-j}(c^*(\alpha))\right|\right\} \tag{4.6}$$

Then put $p^{L-j}(i+1):=c^*(\alpha^*)$ and encode it as $\tilde{p}^{L-j}(i+1):=\alpha^*+i_0$. If there is an interruption or a break take the smallest unused index as the new starting point. When Relaxed EPWT is applied onp^4 , following is path vector and encoded path vectors are obtained:

$p^4=(0,4,8,12,13,14,15,11,7,3,2,1,5,9,10,6)$

$\tilde{p}^4=(0,0,0,0,0,0,0,0,0,0,0,0,0,0,0,0)$

DWT on pixel values toss out following coefficients:

$c^3=(0.4680,0.4230,0.4325,0.4695,0.4415,0.4370,0.4685,0.4325)$

$c^3=(-0.0250,0.0010,-0.0035,-0.005,\ 0.0005,-0.0050,0.0055,-0.0105),$

Repeating the same procedure of interpolation the matrix $\widetilde{c^3}$ is obtained as:

$$\widetilde{c^3}=\begin{bmatrix}0.4680 & 0.4680 & 0.4230 & 0.4230\\ 0.4370 & 0.4685 & 0.4685 & 0.4325\\ 0.4370 & 0.4325 & 0.4325 & 0.4325\\ 0.4415 & 0.4415 & 0.4695 & 0.4695\end{bmatrix}$$

Applying Relaxed EPWT at L=3 gives:

$p^3=(0,1,2,3,4,5,6,7)$

$\tilde{p}^3=(0,0,0,0,0,0,0,0)$

DWT on the path's functional values:

$c^2=(0.4455,0.4510,0.4393,0.4505)$

$g^2 = (0.0225, -0.0185, 0.0023, 0.0180)$

$\widetilde{c^2}$ is obtained after interpolating:

$$\widetilde{c^2} = \begin{bmatrix} 0.4455 & 0.4455 & 0.4455 & 0.4455 \\ 0.4393 & 0.4505 & 0.4505 & 0.4510 \\ 0.4393 & 0.4505 & 0.4505 & 0.4510 \\ 0.4393 & 0.4393 & 0.4510 & 0.4510 \end{bmatrix}$$

Further iteration produces:

$p^2 = (0, 1, 2, 3)$

$\tilde{p}^2 = (0, 0, 0, 0)$

And their coefficient values are:

$c^1 = (0.4483, 0.4449)$

$g^1 = (-0.0027, -0.0056)$

Similarly we have the $\widetilde{c^1}$:

$$\widetilde{c^1} = \begin{bmatrix} 0.4483 & 0.4483 & 0.4483 & 0.4483 \\ 0.4449 & 0.4449 & 0.4449 & 0.4483 \\ 0.4449 & 0.4449 & 0.4449 & 0.4483 \\ 0.4449 & 0.4449 & 0.4483 & 0.4483 \end{bmatrix}$$

Only one wavelet and scaling coefficient is achieved at the end of the algorithm with $c^0 = (0.4466)$ $g^0 = (0.0017)$. Details coefficient of Rigorous EPWT are smaller in magnitude as compared to Relaxed counterpart e.g. $g^0 = (0.00095)$ for Rigorous and $g^0 = (0.0017)$ for Relaxed EPWT, therefore there is a tradeoff in this approach. We can even use combination of Relaxed and Rigorous EPWT. If we take $\phi = 0.02$ path vector p^4 followed is shown in fig.

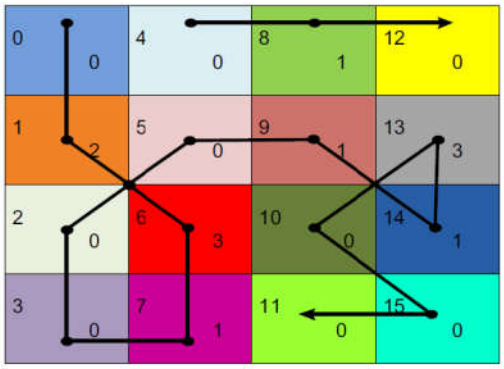

Figure 4.2 EPWT with $\phi = 0.02$

CHAPTER 5
RESULTS AND ANALYSIS

5.1. Introduction

The technique proposed in this research is used to redundancies from the images. This chapter presents step wise experimental results of the proposed algorithm and their analysis. In this research MATLAB R2008a was used as programming environment.

5.2. Input data

Standard bench mark images used in image processing as input data.

5.3. Experiment and Results

Here I will discuss the results of new technique by applying hard threshold on our resultant coefficients, and compare them with Generalized Tree Based Wavelet Transform [12]. First lets discuss lossy and lossless compression.

5.4. Lossless Reconstruction

Standard 'lena' image is shown in fig. 5.1 which is reconstructed from a single scaling and detail vectors. c^8 and g^8 is passed through levels 8 to 14 levels to the reconstructed image Fig. 5.1 (h). Images are zoomed to give a reader a comparable difference when more coefficients are added.

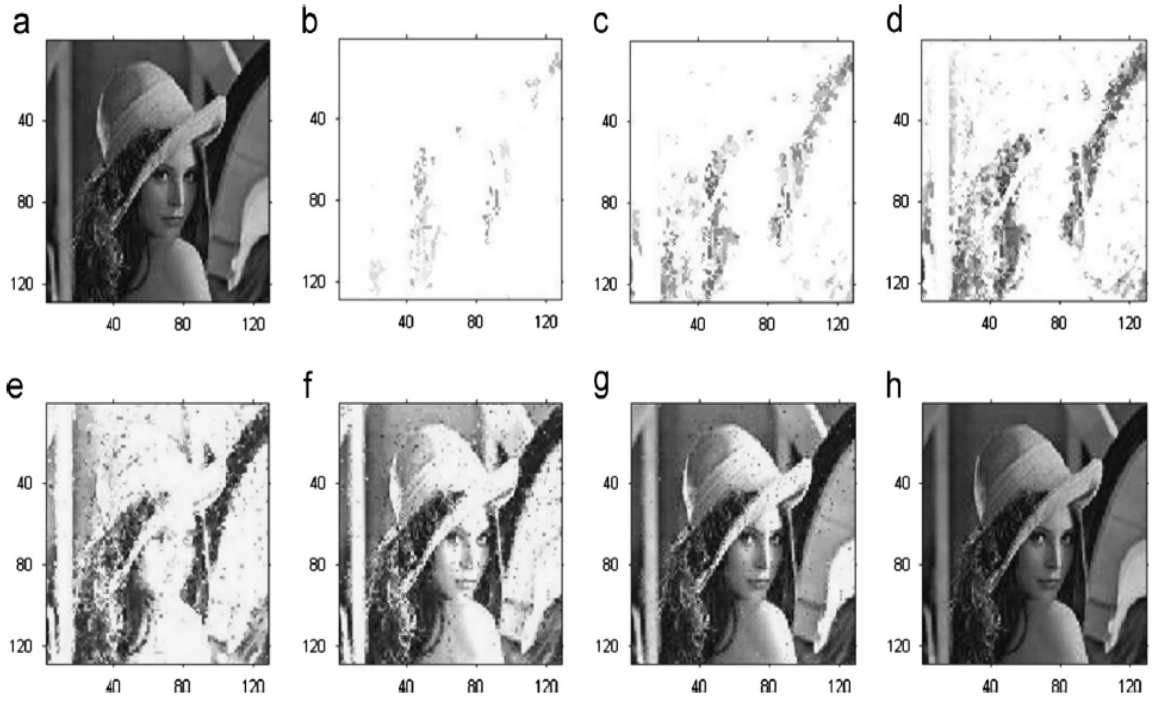

Figure 5.1 Lossless reconstruction with $\phi = \mathbf{0.015}$ (a) Original image, (b–g) Reconstructed levels 8 to 13, (h) reconstructed image 14 level

It must be noted that for reconstruction that all coefficients to be ordered in the same manner in which they were calculated. Since $\log_2(128 * 128) = 14$ therefore fig. 6 needs 7 levels to yield original image. As was discussed in chapter 4, higher threshold leads to more compact path vector or more number of zeroes. Therefore we have a tradeoff between entropy of path and threshold, higher threshold less entropy of path vector and vice versa. Lossless reconstructions of an image using both versions of EPWT are illustrated in figs. 7, 8. Matrix or image used is:

$$c^4 = \begin{bmatrix} 0.4688 & 0.1622 & 0.7656 & 0.7892 \\ 0.5694 & 0.6943 & 0.6020 & 0.9482 \\ 0.0119 & 0.3112 & 0.2630 & 0.6505 \\ 0.2371 & 0.4285 & 0.5541 & 0.3838 \end{bmatrix}$$

We can also see different correlated pixels pairing up in the reconstruction phase also. It is evidently seen from the reconstruction images of fig. 5.2[a-f], 5.3[a-f] the pathways that the pathways followed by both Relaxed and Rigorous EPWT. Trade for Rigorous EPWT is we get low coefficients of details but we have to store the path vectors.

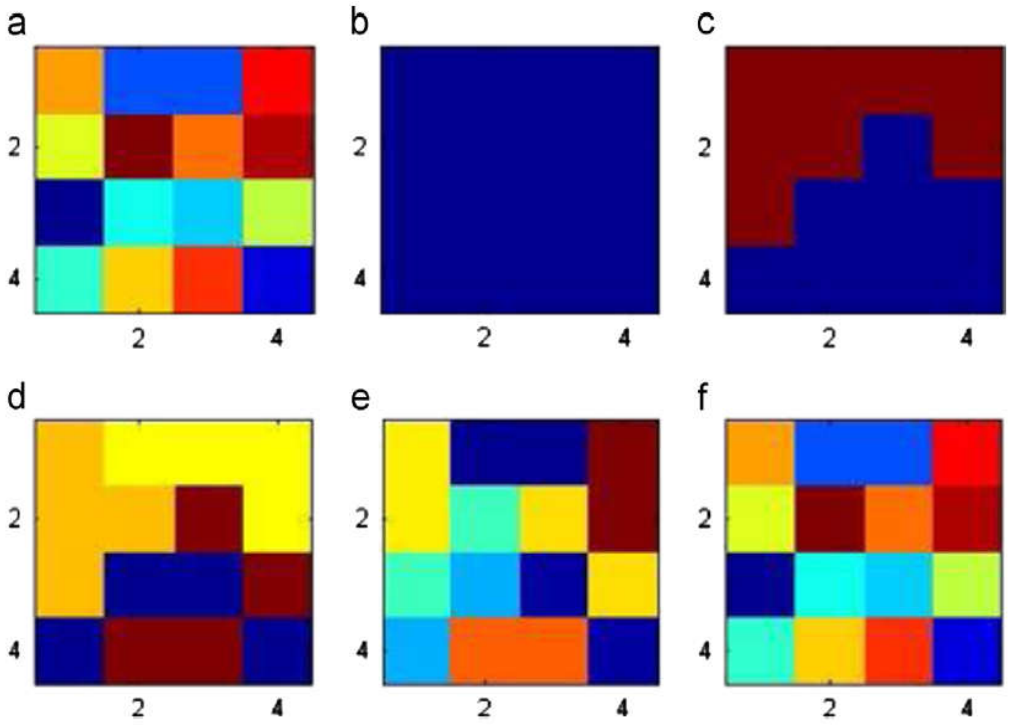

Figure 5.2 Rigorous EPWT reconstruction of c^4 (a) Original frame (b) c^0, (c) c^1, (d) c^2 (e) c^3 (f) c^4

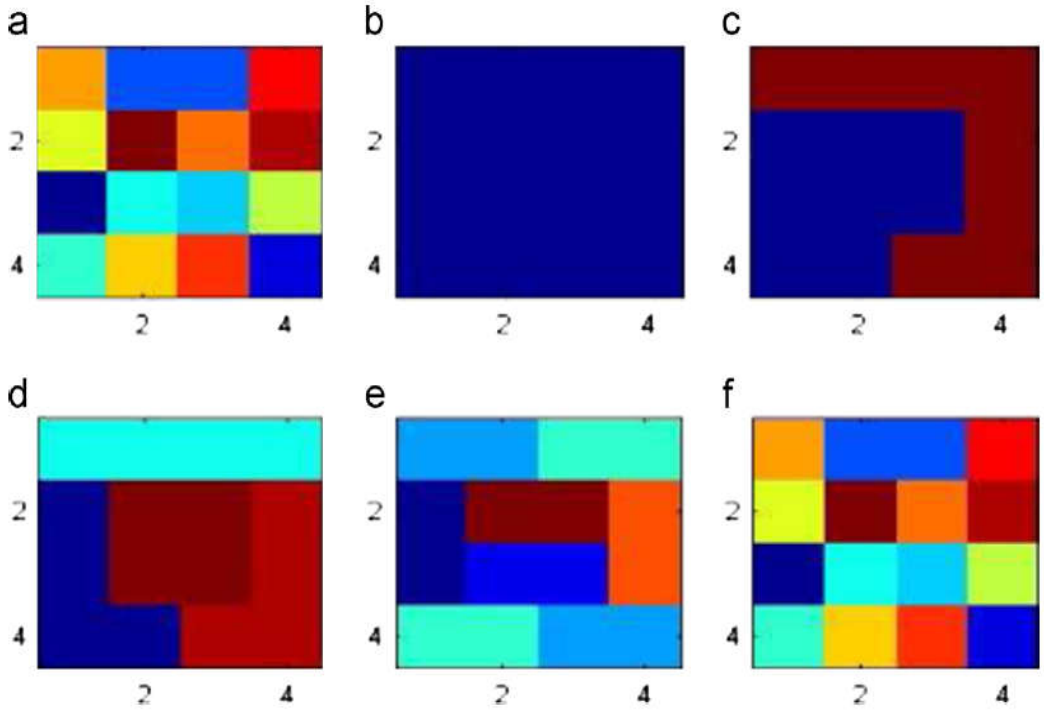

Figure 5.3 Relaxed EPWT reconstruction of c^4 with $\phi = 0.8$ (a) Original frame (b) c^0, (c) c^1, (d) c^2, (e) c^3, (f) c^4

5.5. Lossy Reconstruction

Let's compare EPWT with conventional tensor product wavelet transform or adaptive GTBWT. For this take the standard image of 'house. Fig. 5.4 I have used tensor product Haar, GTBWT and EPWT with different threshold to draw a comparative result of the superior compression. I have used 1024 details coefficients out of total 65536 i.e. compressed the image 64 times. Results expressed are clear indication of the superior compression technique employed.

Relaxed and Rigorous EPWT only differs in the quality of path storage capacity. As EPWT requires storing of encoded path, so we can calculate the efficiency of compression with the help of entropy versus PSNR. For ideal path vectors we must achieve it with minimum entropy and maximum PSNR. As we increase our threshold the entropy decreases. As discussed before number of zeroes increases with increasing threshold as then path followed will be of favorite direction with maximum number of zeroes stored as encoded path vector. This can be seen in fig. 5.5.

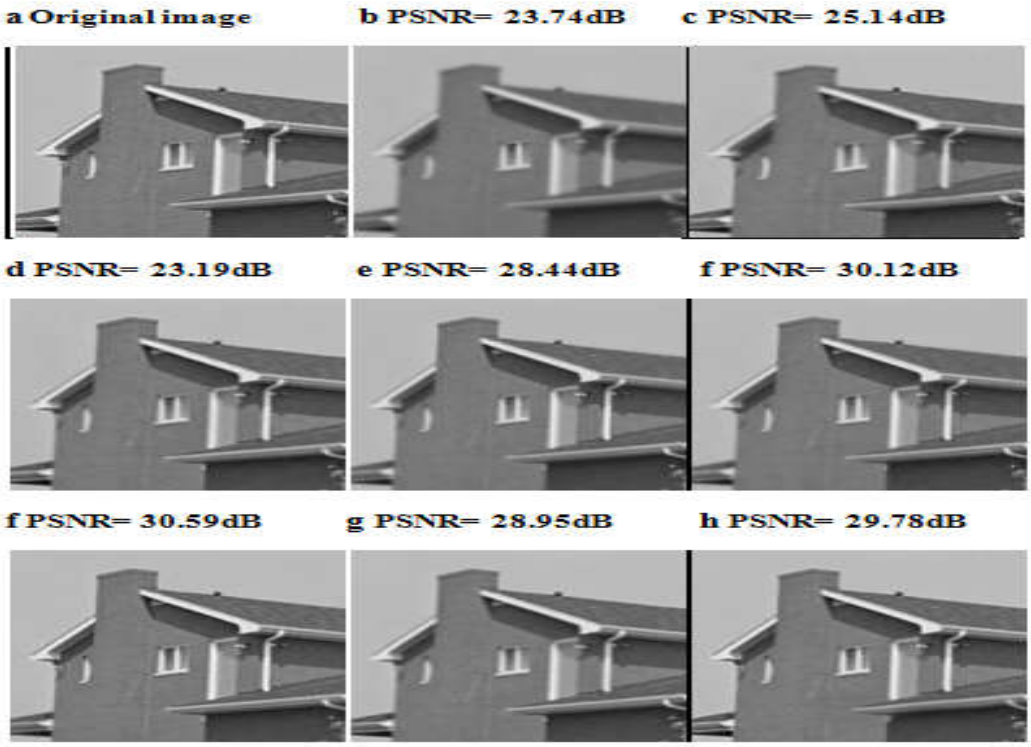

Figure 5.4 (a) House original image, (b) tensor product (Haar), (c) tensor product (db4), (d) GTBWT (Haar), (e) tetrolet 16, (f) EPWT (Haar) $\phi = 0.0$ (g) EPWT (Haar) $\phi = 0.05$, (h) EPWT (Haar) $\phi = 0.1$, and (i) EPWT (Haar) $\phi = 0.15$

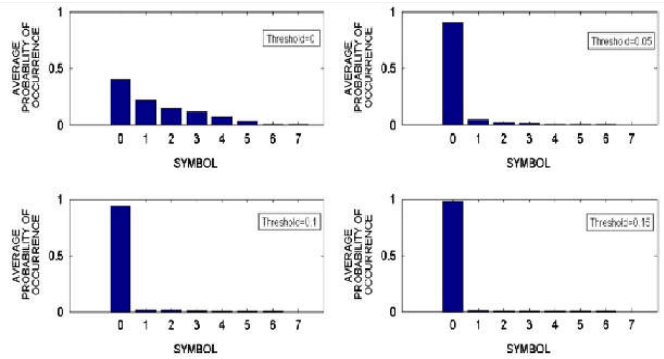

Figure 5.5 Threshold ϕ vs number of '0's

CHAPTER 6

CONCLUSION AND FUTURE WORK

6.1. Conclusion

MRA has been elaborated and implemented on bench images. From above numerical results it can be conclude that selecting an optimal threshold leads to an optimal compression ratio which cannot be calculated rather can be determined by hit and trial method. We also found out a tradeoff between entropy and the threshold. Other compression methods were compared with EPWT with EPWT coming out as a superior technique.

This paper's research can be used for compression of three dimensional video. It can be used for compression satellite video/imagery. Any type of large amount of data can be stored. We can even compress the each individual tensor product wavelet transformed images.

REFERENCES

[1] Rafael C. Gonzalez and Richard E. Woods, —Digital Image Processing‖, 3rd edition, Pearson Education, India, 2008.

[2] Albert Boggess and Francis J. Narcowich, —A First Course in Wavelets with Fourier Analysis‖, Prentice Hall, New Jersey, 2001.

[3] S. Mallat, "A theory for multiresolution signal decomposition: The wavelet representation," IEEE Trans. Pattern Anal. Machine Intell., vol. 11, pp. 674–693, July 1989,

[4] Shapiro, J. (1993). Embedded image coding using zerotrees of wavelets coefficients. *IEEE Trans. Signal Processing* , 3445-3462

[5] Daubechies, I.,Orthonormal bases of compactly supported wavelets,Communications on Pure and Applied Mathematics, Vol. 41, No. 7, pp. 909-996, 1988

[6] A theory for multi-resolution signal decomposition: The wavelet representation, IEEE Transactions on Pattern Analysis and Machine Intelligence, Vol. 11, No. 7, pp. 674-693, 1989.

[7] G. Kaiser, —A Friendly Guide to Wavelets‖, Birkhauser, Boston, 1994.

[8] Gilbert Strang and Truong Nguyen, —Wavelets and filter Banks‖, 4th ed., Wellesley Cambridge Press, 1996.

[9] Alfred Mertins, —Signal Analysis, Wavelets, Filter Banks Time-Frequency Transforms and Application‖, John Willey and Sons, England, 1999.

[10] Truong Q. Nguyen, —A Tutorial on Filter Banks and Wavelets‖, *Proc. Of Intl conf on Digital Signal Processing, Cypress,* June 95.

[11] Stephane G Mallat, —A Theory for Multiresolution Signal Decomposition the Wavelet Representation‖, *IEEE Trans. on pattern and machine intelligence, vol. 11.* 1989.

[12] Idan Ram, Michael Elad, and Israel Cohen, “Generalized Tree-Based Wavelet Transform,” pp. 1–11, Sept. 2011

[13] Erwan Le Pennec and St´ephane Mallat, “Sparse geometric image representation with bandelets,” IEEE transactions on image processing, vol. 14, no. 4, pp. 423–438, 2005

[14] D.L. Donoho, Wedgelets: nearly minimax estimation of edges, Ann. Statist. 27(3), (1999), 859–897. [8] Khalid Sayood ‘Introduction to Data Compression (Morgan Kaufmann, 4th Edition, 2012)

[15] Jens Krommweh, “Tetrolet transform: A new adaptive Haar wavelet algorithm for sparse image representation,” Journal of Visual Communication and Image Representation, vol. 21, no. 4, pp. 364–374, May 2010.

[16] S. Mallat, Geometrical grouplets, Appl. Comput. Harmon. Anal. 26(2) (2009), 161–180.

[17] Syed Akbar Raza Naqvi, Imran Touqir, Adil Masood Siddiqui, “Sparse Representation of Image Video Using EPWT”, in *Signal Processing Journal Vol: pp:- (Journal)*

[18] Y. Meyer, *“*Wavelets: Algorithms and Applications*,‖ Society for Industrial and Applied Mathematics, Philadelphia, pp. 13-31; 101-105*, 1993,

[19] Raghuveer M. Rao and Ajit S. Bopardikar, —Wavelet Transforms,‖ Pearson Education, India, 2004.

[20] Kp. Soman and K. I. Ramachran, —Insight into wavelets‖, 2nd ed., Prentice Hall, India, 2005

[21] Sidney Burrus, Ramesh A. Gopinath and Haito Guo, —Introduction to Wavelets and Wavelet Transforms ‖, Prentice Hall, New Jersey, 1998.

[22] Said, A. (June 1996). IEEE Transactions on Circuits and Systems for Video Technology , Vol. 6